A STUDY OF LINE INTENSITIES IN THE SPECTRUM OF THE STAR ϵ-LEONIS

by

RAY LEWIS FISHER

Bachelor of Science

Oklahoma State University

1954

Submitted to the Faculty of the Graduate School of
the Oklahoma State University
in partial fulfillment of the requirements
for the degree of
MASTER OF SCIENCE
August, 1961

A STUDY OF LINE INTENSITIES IN THE SPECTRUM

OF THE STAR ϵ- LEONIS

Thesis Approved:

Leon W. Schroeder

Thesis Adviser

Benjamin Rock

Louis Madison

Dean of the Graduate School

PREFACE

This work was undertaken at the suggestion of Dr. L. W. Schroeder who acted as my adviser. The purpose of the paper is to contribute some information concerning the stellar atmosphere of a solar type star.

The star chosen for the study is ϵ -Leonis. This star has the coordinates $\alpha(1900) = 9^h\ 40.2^m$, $\delta(1900) = +24^\circ\ 14'$. The spectral type is G0 and luminsoity class II. It is listed in the Henry Draper catalog as Number 84441. Visual magnitude is m = 3.26.

Dr. Schroeder's advice and assistance have been invaluable in the completion of my work. This has been greatly appreciated. The assistance of the Research Foundation is also appreciated.

The work was carried on under NONR contract number (G)-00017-61. This support is gratefully acknowledged.

The author is also indebted to the Dominion Astrophysical Observatory and particularly to Dr. K. O. Wright, of that institution, for the furnishing of the spectrograms and tracings upon which this study is based.

TABLE OF CONTENTS

LIST OF TABLES

LIST OF FIGURES

LIST OF FIGURES (Continued)

I. INTRODUCTION

This paper is concerned with the analysis of the stellar atmosphere of ϵ-Leonis by means of curves of growth, a method termed "grobanalysis" by German workers.

Curves of growth have been used extensively since Menzel (1936) first developed the theory as applied to the Schuster-Schwarzschild model atmosphere. Wrubel (1949, 1950, 1956) has made use of Chandrasekhar's exact solution of the equation of transfer for the Milne-Eddington model atmosphere to calculate theoretical curves of growth for both pure scattering and pure absorption. He has further (1954) applied the same technique to calculate theoretical curves for the Schuster-Schwarzschild model, pure scattering. Pure absorption curves for this model have been calculated by Hunger (1956).

An exact model atmosphere for a given star cannot be readily assumed nor the exact mechanism of radiative transfer known. Hence we are forced to deal with approximations for both. The two extreme approaches to stellar atmospheres are represented by the Schuster-Schwarzschild and Milne-Eddington models. (Henceforth these shall be known as the S-S and M-E models, respectively.) The extremes of radiation transfer are pure scattering and pure absorption. Thus a complete analysis will consist of four curves of growth for each element under consideration.

This study has been limited to lines of Fe I, Ti I, and Cr I. The wavelength range covers $\lambda\lambda$ 4000-5450. It was decided to use only those

lines for which the laboratory f-values are known. It is generally felt that the laboratory f-values are considerably more reliable than those calculated from theory. The wavelength restriction was made to avoid the more complex ultra-violet spectra and the wings of the H and K lines of Ca I.

Using those lines sufficiently free of blending and with high enough resolution, equivalent widths of one hundred and seven lines of neutral iron, titanium, and chromium were measured, based upon a total of two hundred and thirty-five measurements. Excitation temperatures and abundances for each element were found for the cases of pure scattering and pure absorption for both the S-S and M-E models.

II. CURVE OF GROWTH ANALYSIS

The curve of growth is defined as the relation between the intensity of an absorption line and the number of absorbing atoms. These quantities may be directly observed in the laboratory.

The quantity upon which the observed curves of growth are based is the equivalent width of an absorption line. To obtain this, it is assumed that the continuum is a constant over the region of a single line, and has an intensity of unity. Then the intensity at a point on the line is given by R. The shape of the profile is considered to be a function of wavelength. The total energy absorbed is given by the area enclosed by the profile and the continuum.

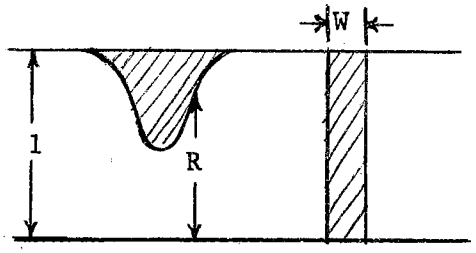

Figure 1. The Equivalent Width, W, of a Spectral Line

Now if one replaces this profile by a rectangle having the same area and of unit height, the width of the rectangle is known as the equivalent width. It is normally expressed in milliangstroms.

The advantage of the equivalent width is that it is less affected by the finite resolution of the spectrograph than is the line profile. It is also relatively free of the Doppler effects of stellar rotation and macro-turbulence. The usefulness of the curve of growth lies in the fact that it is based upon this single observational datum.

Other methods of analysis, such as detailed studies of line profiles and calculations of model atmospheres yield more definitive data than a curve of growth analysis, which is a statistical procedure, but they will not be attempted here. However the curve of growth has been a most useful tool in the study of many stellar atmospheres and can be used as a basis for the more refined techniques.

A laboratory curve of growth may be found by varying the concentration of atoms in an absorption tube and measuring the strength of the lines produced when light from an incandescent source passes through the tube. The equivalent widths are then determined for the lines of the element under investigation. The curve of growth is found by plotting the logarithm of the equivalent width versus the logarithm of the number of absorbing atoms. The number of effective absorbers (Nf) is found by the product of the total number of atoms and the f-value or oscillator strength of the line in question.

Looking at the curve of growth, it is seen that at the outset (that is for W small or for the weakest lines) there is nearly a linear relationship between W and Nf. However as the number of absorbers increases the line becomes saturated and there is only a very small increase in equivalent width with a large increase in the number of absorbers. This point at which the linearity of the relation ceases and the curve becomes "flat" is known as the "knee" of the curve. The curve then remains nearly horizontal until the damping portion is reached. From this point the principal contribution to the equivalent width is the development of the "wings" of the line and W is proportional to the square root of Nf.

The preceding discussion is based upon a constant temperature. If there is a variation in temperature the position of the knee will change.

A higher temperature results in a greater Maxwellian velocity distribution of the absorbing atoms. Hence the line will be broader and the knee of the curve higher. It should also be noted that the position of the knee has been found to depend upon the turbulence in the stellar atmosphere.

If one designates the velocity of the atom by V, the thermal velocity by V_o and the velocity due to turbulence by V_T, we have the relationship;

$$(1) \quad V^2 = V_o^2 + V_T^2$$

Thus the average velocity of an absorbing atom is much higher than would be found by using the effective temperature of the star. The effect of turbulence is, then, to force us to fit our observed curve of growth to a theoretical curve indicative of a temperature considerably higher than that called for by the effective temperature.

The second part of Figure 2 shows the effect of damping on the curve of growth. For a given temperature increased damping results in less flat portion of the curve. Then for large damping there is practically a smooth blending from the linear portion of the curve to the damping portion. Formation of the wings begins earlier with respect to the effective number of absorbers. The smaller the damping the more flat portion in the curve from the knee to the point where damping begins. For this case there must be a considerable increase in the number of absorbers before damping begins.

In the observed curve of growth one must work backwards from the laboratory approach. From the observed intensities one finds the equivalent widths and from this single observation arrives at the abundances and excitation temperatures of the various elements desired.

In the laboratory experiment a reasonable assumption of a constant temperature within the absorption tube was made. However in stellar

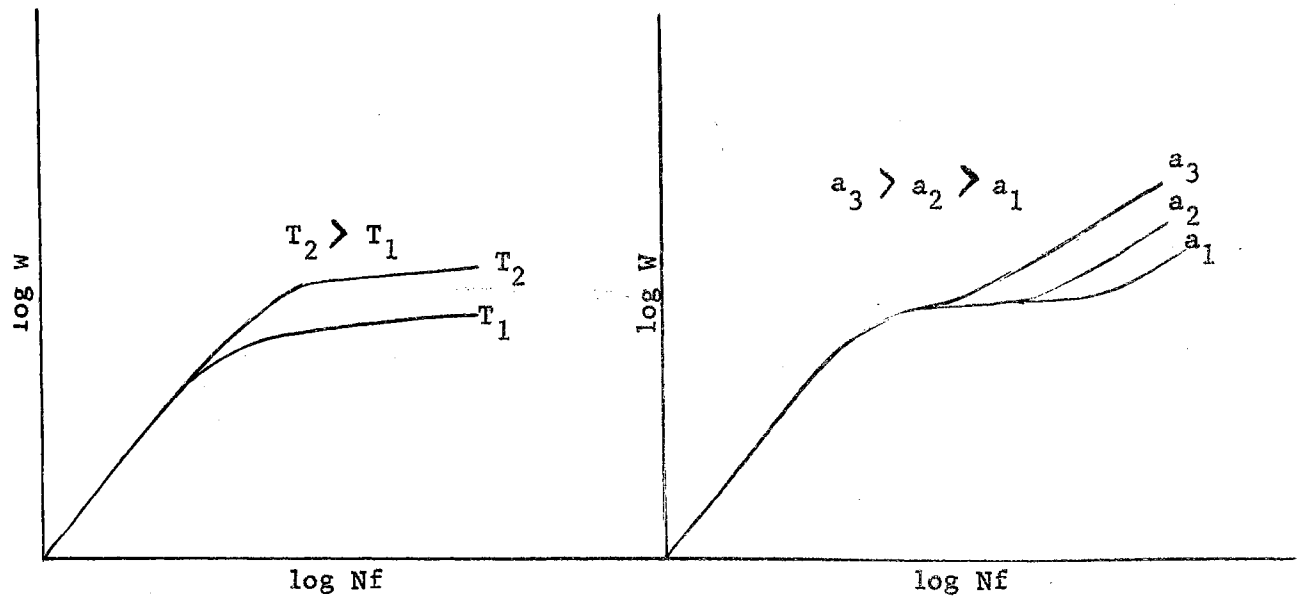

Figure 2. Effect of Temperature and Damping on the Curve of Growth

atmospheres we find that the temperature increases approximately as $\tau^{1/4}$ where τ is the optical depth. Obviously, some sort of reconciliation must be made with an assumption of a constant temperature or nearly so. To do this we assume that the line is effectively formed at some given layer within the atmosphere and thus that the temperature and other properties of that level are associated with the line.

This, of course, is only an approximation and hardly could be expected to hold for all lines. Some notable exceptions to this are weak lines and the wings and center of strong lines. For weak lines and the wings of strong lines there is little absorption and we see more deeply into the atmosphere. Thus a higher temperature is associated with this formation. At the core of strong lines there is considerable absorption implying that we see only into the upper layers of the atmosphere where the temperature is lower.

However if one considers the relative amount of contribution from the various portions of the atmosphere he finds that the original

assumption will not be too much in error. With this in mind, then, consider the formation of non-resonant lines of neutral atoms. First, in the upper atmosphere the temperature is low and atoms there will have a low level of excitation resulting in small contributions to the lines in question. Deeper in the atmosphere the temperature will have increased to a point where there is high excitation and ionization has begun. The contribution from such levels will again be small. Thus for non-resonant lines of neutral atoms, the lines are essentially formed in the intermediate levels.

Earlier it was mentioned that the S-S and M-E models represented the extremes in models of stellar atmospheres. A comparison of the two models might now be appropriate.

The S-S Model:

This model assumes a photosphere which produces a continuous spectrum with a so-called "reversing layer" of finite optical depth above it where the lines are formed. The optical depth of this layer is a function of the absorption coefficient of the line. It is considered that no continuous absorption occurs here but rather that the transmitted portion of the radiation from the photosphere is subjected to selective absorption and scattering. A part of the radiation from below is reflected back to the photosphere where there is continuous absorption. The formation of the wings of the line are considered to be due to the small optical thickness of the reversing layer compared to the thickness at the line core. This model is a good approximation for lines formed well above the photosphere and is quite representative of the neutral metals. Here the number of absorbers decreases with optical depth, since as the temperature increases more and more ionization occurs.

The M-E Model:

This model, as opposed to the S-S model, assumes that the lines and continuum are formed in the same region. Also, the ratio of the line absorption coefficient to the continuous absorption coefficient ($l_\nu/k_\nu = \eta_\nu$) is constant with depth for each frequency. While l_ν and k_ν may change independently their ratio must remain the same. It is considered that the line wings result from few absorptions and reemissions while at the line core there are many absorptions and reemissions and the photon may be "lost".

Strömgren (1937) has found in some cases that the variation of line to continuous absorption with depth is small enough that an average value may be used for layers important in the formation of absorption lines. For such cases, then, the M-E model is a good approximation.

Comparing the two models one sees that although their approach is quite different, they have in common that a selective process in the formation of the line is followed by continuous absorption.

As previously mentioned the extremes in radiation transfer are pure scattering and pure absorption. Scattering is of two types. If the energy is absorbed and reemitted at a single frequency the scattering is said to be coherent. If the incident energy is reemitted over a narrow band of frequencies, it is non-coherent scattering. In the case of absorption there is no general relation between incident and emitted frequencies. Here the energy is absorbed and then given off in a number of possible ways dependent only upon the temperature.

Under idealized conditions a wealth of data may be obtained from the curve of growth. A description of these conditions and the data which would result from their satisfaction follows.

If, 1) the atmosphere were built on either the M-E or S-S model,

2) it were in theromdynamic equilibrium at a temperature T which is constant throughout the atmosphere,

3) turbulence were negligible,

4) the effects of broadening were constant with depth,

5) measurements from a single level were available,

6) ϵ_ν, the ratio of line scattering to line absorption were known and constant with depth, and,

7) absolute f-values were known,

then

1) the temperature could be determined,

2) the abundance of the element could be determined, and

3) Γ_c, the collisional damping constant, could be found, all from the curve of growth.

That these conditions are not met in stellar atmospheres is obvious. The departure from the ideal correspondingly limits the reliability of the information obtained.

Now assume one has obtained measured equivalent widths and wishes to reduce this data to the desired quantities. For this purpose assume the simplest case, that is that there are many lines arising from a single level, and that the absolute f-values for all the lines are known.

The relation between the equivalent width and the residual intensity R, is

$$(2) \quad \frac{W}{b} = \int_{-\infty}^{+\infty} (1-R)\,dv .$$

W is the equivalent width and b is the Doppler width of the line.

$$(3) \quad b = \frac{\lambda v}{d} \text{ where } V = \sqrt{\frac{2kT}{m}} .$$

In the expression for v, k is Boltzmann's constant, m the atomic mass and T is the kinetic temperature. In the expression for the Doppler width λ is the wave length and c the velocity of light.

In the integral, R is the residual intensity at a point in the line with respect to a continuum intensity of unity and may be found from the equation of transfer. The quantity v is the deviation from the center of the line in units of Doppler width. Then $v = \frac{\lambda - \lambda_o}{b}$. R is calculated somewhat differently in the two models. The M-E model has R as a function of the ratio η_o ($\eta_o = \ell_o / \kappa_o$: ℓ_o = scattering coefficient and κ_o the absorption coefficient at the center of the line). For the S-S model R is a function of the fictitious optical depth at the center of the line, τ_o.

The theoretical curves used in this paper assume that the Planck function $B_\nu(T)$ is linear with optical depth. Then $B_\nu(T) = B^o + B^1 \tau_\nu$. For the S-S model this leads to $I = I^o + I^1 \mu$, where $\mu = \cos\theta$, and the equation represents a limb darkening law in the continuum. $I = B^o + B^1 \mu$ for the M-E model. Investigation by Hunger (1956) has shown that further terms are unnecessary.

The theoretical curve of growth for the S-S model would then be a plot of $\log \frac{W}{b}$ versus $\log \tau_o$. There is the relation

$$(4) \quad \tau_o = \int \kappa_o \eta \, d\ell$$

where κ_o is the fictitious absorption coefficient at the line center per oscillator and η is the number of classical oscillators per unit volume. However, we have that $\eta = N_n f_{nj}$, where N_n is the number of atoms in level n per unit volume and f_{nj} is the f-value or probability of a transition from level n to level j. Then substituting and integrating we have $\tau_o = \kappa_o N_n f_{nj} H$ and H is the height of the reversing layer. Then the

product $N_n H$ is the number of absorbers in level n in a column of one square centimeter through the entire atmosphere. Substitute for K_o,

$$(5) \quad K_o = \frac{\pi^{1/2} e^2 \lambda^2}{mc^2 b}$$

where b, λ, and c are as defined previously. In this expression m is the mass of the electron, and e the electron charge. Then express K_o as $K_o = C \frac{\lambda}{v/c}$ where $C = \frac{\pi^{1/2} e^2}{mc^2}$. Making this substitution $\tau_o = (C \frac{\lambda}{v/c}) N_n H f$. Taking the log of this equation

$$(6) \quad \log \tau_o = \log N_n H + \log C + \log f\lambda + \log c/v.$$

Since it was assumed the equivalent widths have been measured and the absolute f-values known, plot $\log \frac{W}{\lambda}$ versus $\log f\lambda$ on transparent paper. Fit the observed curve on the theoretical curve by <u>only</u> horizontal and vertical shifts. There should be <u>no</u> rotation of axes.

The vertical shift of the curve then yields $\log c/v$. From the horizontal shift we have

$$\log \tau_o - \log f\lambda = \log N_n H + \log C + \log c/v$$

Log C may be evaluated and $\log c/v$ has been determined from the vertical shift. Thus

$$\log N_n H = \text{shift} - \log C - \log c/v$$

The situation described above is not that usually met in observations. One must deal with multiplets, lines arising from several levels within a term. In this case apply the Bolzman equation,

$$(7) \quad \frac{N_n}{N} = \frac{g_n}{U} \exp(-\chi e/kT).$$

Here N is the total number of atoms, g_n is the statistical weight of level n($g_n = 2J + 1$), U is the partition function, $U = \Sigma g_i W \exp(-\chi e,i/kT)$ summed over all levels in the atom (W is a correction for pressure effects), T is the excitation temperature, and χe is the excitation potential of the lower level in electron volts.

Then in the case of multiplets, one plots as the abscissa for the observed curve log ($gf\lambda \exp -\chi_e/kT$) = log $gf\lambda - \theta\chi_e$. Here $\theta = \frac{5040}{T}$. Log W/λ remains the ordinate. The constant "C" which occurs in the expression for the theoretical curve's abscissa, in this case, contains the partition function as well as the $\theta\chi_e$ term. The abundance is found in much the same manner as before, with the above modifications in the equation.

What was termed the total number of atoms, above, is in reality only the total number of neutral atoms of the given element. Abundances of atoms of various stages of ionization may be found from the Saha equation. In logarithmic form this is

$$(8) \quad \log \frac{N_1}{N_o} = - \log p_e - \theta \chi_i + 2.5 \log T - 0.48 + \log \frac{2U_1}{U_o}$$

where N_1 is the number of atoms in the first stage of ionization per unit volume, N_o the number of neutral atoms per unit volume, p_e is the electron pressure in dynes/cm^2, χ_i is the ionization potential, T is the ionization temperature, U_1 is the partition function for the ionized atoms, and U_o the partition function of the neutral atoms. If one wishes the abundances for several levels of ionization the Saha equation is to be applied successively for each level desired. In this paper it is found that abundances for doubly ionized atoms were small enough to be neglected.

The abscissa for the M-E curves of growth is $\log \eta_o$. As will be shown one obtains from this log $N/\rho\bar{K}$, where N/ρ represents the number of absorbing atoms per gram and $1/\bar{K}$ represents the number of grams of stellar material in a square centimeter column in which the line is formed. $\bar{K}$ is the mean continuous absorption coefficient per gram of stellar material.

Some corrections are necessary in the observed curves of growth. The corrections, $\Delta \log \eta_o$ or $\Delta \log \tau_o$, are functions of limb darkening and

W/b. These corrections are made with regard to the variation of limb darkening with wavelength. The corrections are derived from theoretical curves of growth. These corrections will be discussed later in the paper.

As a summation of the discussion of curves of growth, in general, a brief outline of the steps in the curve of growth technique follows.

1) Use spectra of the highest dispersion available. For such spectra the blending is cut to a minimum due to the increased resolution.
2) Obtain microphotometer tracings of the spectra. The microphotometer tracing is linear in the density of the image but not in intensity.
3) Obtain intensitometer tracings. This step converts the density of the image to intensity. Calibration is made from sources of known intensity.

Note should be made that, while the above steps are performed separately at the Dominion Astrophysical Observatory, two steps (2 and 3) are combined at some observatories and work is being done toward the combination of all three. This work is being carried on by Code, Stromgren, and Hiltner.

4) Draw in the continuum. In most cases the continuum was drawn directly on the intensitometer tracings. In some cases it was first drawn on the microphotometer tracings and then transferred. This step involves, probably, the greatest single source of error.
5) Identify lines and draw the profiles. Where possible comparison of more than one plate will aid in determining the general shape and position of a profile. All profiles were drawn as proportional to $1/\nu^2$, as theory suggests, rather than as triangles as some workers have done.

6) Determine equivalent widths. After the profiles were drawn the area enclosed by the profile and the continuum was measured with a planimeter. The continuum height was taken as the mean of the heights on both sides of the profile.

7) Plot log $gf\lambda$ versus log W/λ for the lines of the same term. That is plot each multiplet on separate sheets.

8) Fit the observed multiplet plots together, to form a smooth curve. Horizontal shifts only are made in this fitting. The horizontal shift is then plotted as a function of the average excitation potential of the multiplets. The slope of the resulting straight line is proportional to θ and hence the excitation temperature may be found.

9) Match observed and theoretical curves of growth. The vertical shift gives log c/ν. From the horizontal shift one finds the abundance of the atom or ion in question, using the log c/ν of the vertical shift.

Steps 7, 8, and 9 must be repeated for each element and each ion of the element for which results are desired.

10) Apply the Saha equation as many times as necessary to obtain the total abundance of each element.

III. OBSERVATIONAL MATERIAL

The spectrograms used in this study were taken at the Dominion Astrophysical Observatory by Dr. K. O. Wright. The 72 inch telescope was used with the spectrograph at the Cassegrain focus.

The dispersion varied, depending upon the spectrograph used. For the Littrow spectrograph with the Wood grating (15,000 lines/inch) the dispersion was approximately 7.5 A/mm for second order spectra in the range $\lambda\lambda$ 4800-6750; for third order spectra in the range $\lambda\lambda$ 3750-4500, the dispersion was about 4.5 A/mm. When the Bausch and Lomb grating No. 496 (30,000 lines/inch) was used in the second order, the dispersion was about 3.2 A/mm. For the three-prism spectrograph the dispersion varied from about 5 A/mm to 15 A/mm over the wavelength range studied.

Dr. L. W. Schroeder made the microphotometer and intenstometer tracings at Victoria and furnished those used in this study. Table I shows the details of the data just described. Samples of representative spectra are shown in Plate I.

As mentioned earlier, in most cases the continuum was drawn directly on the intensitometer tracings. It was assumed that the continuum was given by the average galvanometer deflections, due to plate grains, between lines. Several such points were chosen along the intensitometer tracings and a straight line drawn through the points. Where possible a single line was drawn across the entire tracing representing the continuum.

TABLE I

VICTORIA PLATE, MICROPHOTOMETER, AND INTENSITOMETER DATA FOR ϵ-LEONIS

Victoria Plate Number	Microphotometer & Intensitometer Tracing Number	Spectrograph	Wavelength Range (Angstroms)
55222	1802	Grating*- 2nd Order	3890-4100
38155	1821	Grating- 2nd Order	3900-4110
38155	1820	Grating- 2nd Order	4100-4255
38299	1823	Grating- 3rd Order	4030-4250
55223	1795	Grating- 2nd Order	4170-4315
30041	1801	Prism	4200-4555
55223	1794	Grating*- 2nd Order	4325-4490
36853	1813	Prism	4550-4920
31388	1805	Prism	4610-5060
35857	1826	Grating- 2nd Order	5130-5500
31388	1804	Prism	5000-5700
38106	1825	Grating- 2nd Order	5400-5720

*The asterisk refers to grating spectra made with the Bausch and Lomb grating No. 496. All other grating spectra were made with the Wood grating. Prism spectrograms were made with the three prism spectrograph.

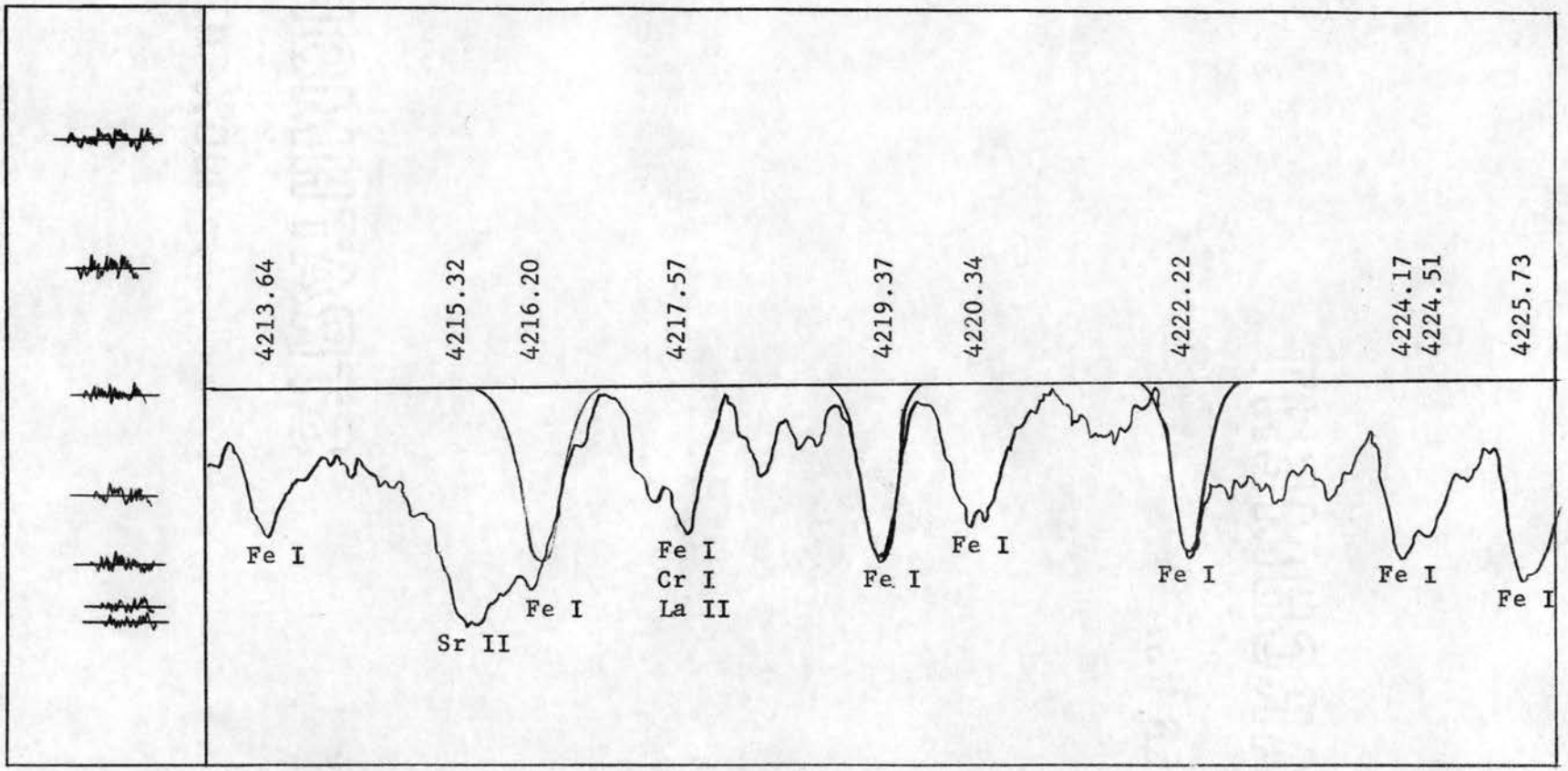

Figure 2a. Microphotemeter Tracing of the Spectrum of ϵ- Leonis. The region shown is $\lambda\lambda$ 4213-4226. a line has been drawn indicating the estimated position of the continuum and three representative profiles are drawn for lines whose equivalent widths were measured. The intensity ratio between steps shown at left of the figure is 1.58. Wavelengths and identification have been marked. Linear magnification is 100.

Plate I

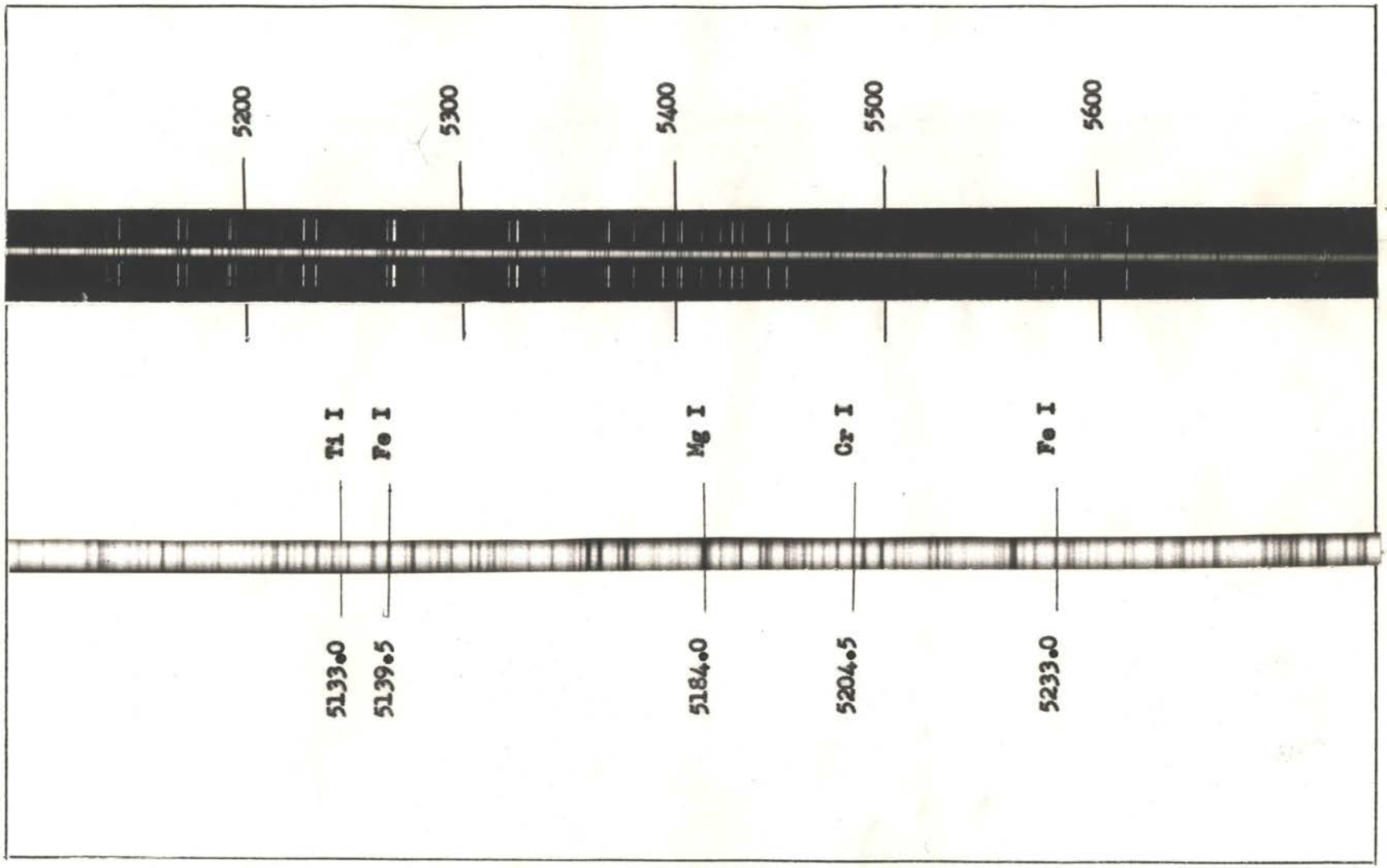

Representative Spectra of ϵ-Leonis.
Wavelengths (Angstroms) and identifications are shown for representative lines.

In some cases, a change of slope was necessary in order to better fit the assumption of the continuum location.

Identification of the lines was made by comparison with intensitometer tracings of Procyon along with Swensson's (1946) tables in his paper on "The Spectrum of Procyon". Swensson's tables were primarily used to check for blending of lines. His listed wavelengths were corrected to the values given in A Multiplet Table of Astrophysical Interest, Revised Edition (RMT) by Charlotte E. Moore (1946). An attempt was made to draw the profiles proportional to $1/\nu^2$.

Measurement of the areas enclosed by the profiles and the continuum was made by two trials each of two circuits with the planimeter. The mean value of the areas was then divided by the mean height of the continuum above the line giving the equivalent width. The dispersion was measured at several points and plotted as a function of wavelength for each tracing. A straight line fit was made to obtain the dispersion and equivalent widths were converted to mA. Profiles were measured only for those lines used in this study. Lines were chosen with regard to the limitations set forth earlier in this paper. Since there was considerable overlapping in the spectral regions of the plates, as many as four values of the equivalent widths of some lines were determined. In some cases only one measurement was possible while most had two measurements. An average for all measurements of the equivalent widths of a line was used for the value of the equivalent width of that line. This procedure would seem to be justified by plotting log W measured on the various plates for each line against each other. The results of this plot are shown in Figure 3.

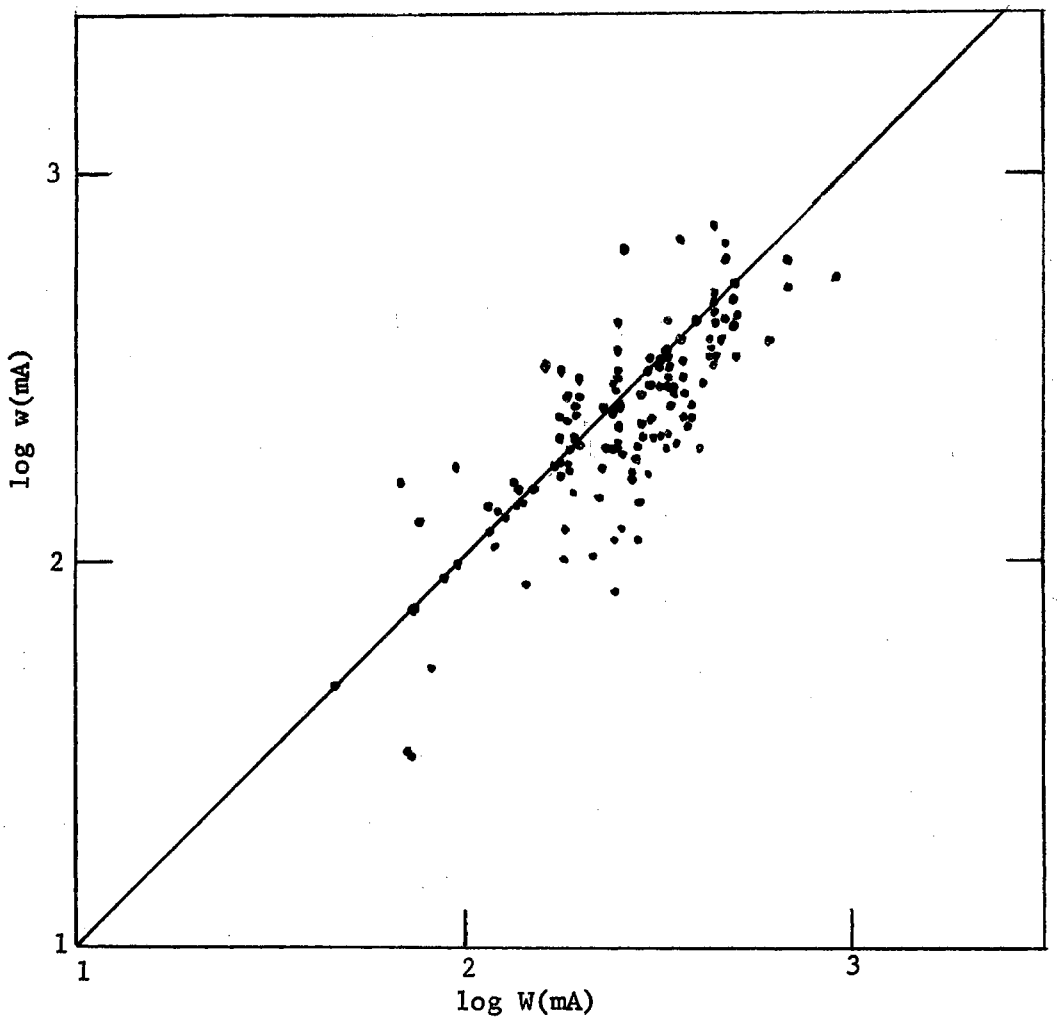

Figure 3. Comparison of Equivalent Widths Measured on Different Tracings

Three lines were measured on the wings of the Hγ line in the Balmer series of hydrogen. Here the measured equivalent width was made with regard to the wing as the continuum. The total equivalent widths of these lines were found with the relation given by Thackeray (1936). If W_b is the equivalent width measured as given above, and r_w is the intensity of the wing at the center of the measured line, then the total equivalent width is given by

$$W = W_b / r_w .$$

Equivalent widths of 58 lines of Fe I, 33 lines of Cr I, and 16 lines of Ti I were measured. Results of these measurements are shown in Table II along with other pertinent data used in obtaining the observed curves of growth. An explanation of the table follows.

Table II: Data for each element is listed according to increasing atomic weight.

Column 1 gives the wave length as given by the Revised Multiplet Table.

Column 2 gives the multiplet number from the Revised Multiplet Table.

Column 3 lists the excitation potential of the lower level of the atomic transition in volts.

Column 4 gives the logarithm of the product of gf times the wavelength. For Ti I the Kings (1938) values for the relative f-values were used. For Cr I the values given by Hill and King (1951) were used. Data for Fe I is separated into two parts. The first is for lines for which the Kings (1938) relative f-values were used. Reference to these lines will be made by Fe I-King. For the other Fe I lines the absolute f-values of Carter (1949) were used. These lines will be referred to as Fe I-Carter.

Column 5 gives the number of measures for each line (i.e., the number of tracings on which it appears).

Column 6 lists the central intensities of the strongest lines. R_c here is Hunger's notation and should not be confused with the residual intensity defined earlier. The residual intensity may be found by subtracting the value listed here from unity. This data is used in the S-S pure absorption curves of growth.

Column 7 gives the equivalent widths in milliangstroms. The equivalent widths of lines on the hydrogen ($H\gamma$) wing are indicated by asterisks.

Column 8 lists the logarithms of the equivalent widths divided by the wavelength.

Column 9 gives the ratio of the limb darkening coefficients for each line. Since the effective temperature of ϵ-Leonis is in the neighborhood of that of the sun the values of B^o/B^i were taken to be the same as the solar values listed by Houtgast (1942). In other words the origin of the continuous opacity was assumed to be the negative hydrogen ion. The temperature of ϵ-Leonis is sufficiently low that the effects of neutral hydrogen and helium would make only a slight contribution to the continuous absorption in the atmosphere.

Column 10. - The theoretical curves used were all based upon a value of 2/3 for B^o/B^i. Hence all values of B^o/B^i must be reduced to 2/3 for comparison with a single curve of growth. This was accomplished by making the corrections listed here. The values listed were found by interpolation in the various published curves of growth. The corrections for the S-S model $\Delta \log \tau_o$ were found to be negligible.

TABLE II

LINE INTENSITIES IN THE SPECTRUM OF ϵ-LEONIS

	λ RMT	Multiplet (RMT)	χ_e	log gfλ	Number of Measures	R_c	W (MA)	log $\frac{W}{\lambda}$	B^0/B^1	Δ log η_o Scattering	Δ log η_o Absorption
Ti I	4008.926	12	0.02	-2.22	2	0.487	256.3	-4.19	0.29	0.13	0.28
	4286.006	44	0.82	-1.48	2	0.502	243.8	-4.25	0.33	0.11	0.25
	4287.405	44	0.83	-1.48	2		114.0	-4.58	0.33	0.14	0.41
	4305.901	44	0.84	-0.70	2	0.653	589.2	-3.86	0.33	0.11	0.23
	4518.022	42	0.82	-1.47	1		172.7	-4.42	0.36	0.10	0.26
	4533.238	42	0.84	-0.64	1	0.430	304.7	-4.17	0.37	0.10	0.22
	4534.782	42	0.83	-0.80	1		248.7	-4.26	0.37	0.10	0.23
	4623.098	145	1.73	-1.11	2		97.81	-4.67	0.38	0.12	0.46
	4656.468	6	0.00	-2.49	2		178.6	-4.42	0.39	0.09	0.23
	4681.908	6	0.05	-2.21	2	0.472	398.7	-4.07	0.39	0.09	0.20
	4981.732	38	0.84	-0.59	1		198.6	-4.40	0.44	0.08	0.18
	5016.162	38	0.84	-1.64	1		189.8	-4.42	0.45	0.07	0.18
	5024.842	38	0.81	-1.69	1		89.49	-4.75	0.45	0.10	0.41
	5039.959	5	0.02	-2.17	1		156.1	-4.51	0.45	0.08	0.22
	5173.742	4	0.00	-2.16	2		230.4	-4.35	0.48	0.06	0.15
	5210.386	4	0.05	-1.90	2		191.1	-4.44	0.48	0.06	0.17
Cr I	4120.613	65	2.70	-0.57	2		68.22	-4.78	0.30	0.17	0.73
	4254.346	1	0.00	-1.37	4		295.2	-4.16	0.32	0.12	0.27
	4272.910	96	2.89	-0.61	2		46.81	-4.96	0.33	0.13	0.51
	4274.803	1	0.00	-1.48	2	0.702	329.9	-4.11	0.33	0.11	0.25
	4289.721	1	0.00	-1.62	2	0.722	417.3	-4.01	0.33	0.11	0.25
	4337.566	22	0.96	-1.80	2		223.4*	-4.29	0.33	0.11	0.28
	4344.507	22	1.00	-1.43	2		301.0*	-4.16	0.34	0.11	0.26
	4346.833	104	2.97	-0.27	2		170.0	-4.41	0.34	0.11	0.33
	4381.112	64	2.70	-0.68	2		52.20	-3.92	0.34	0.11	0.24

TABLE II (Cont'd)

	RMT	Multiplet (RMT)	χ_e	log gfλ	Number of Measures	R_c	W (MA)	log $\frac{W}{\lambda}$	B^0/B^1	$\Delta \log \eta_o$ Scattering	$\Delta \log \eta_o$ Absorption
	4387.496	103	2.99	-0.41	2		115.8	-4.58	0.34	0.14	0.55
	4545.956	10	0.94	-1.99	1		176.5	-4.41	0.37	0.10	0.30
	4591.394	21	0.96	-2.27	1		130.1	-4.55	0.38	0.12	0.45
	4600.752	21	1.00	-1.85	1		239.7	-4.28	0.38	0.10	0.23
	4616.137	21	0.98	-1.90	1		152.5	-4.48	0.38	0.10	0.37
	4626.188	21	0.96	-1.89	2		146.8	-4.50	0.38	0.11	0.39
	4646.174	21	1.03	-1.45	2		211.6	-4.34	0.39	0.09	0.25
	4651.285	21	0.98	-2.00	2		128.3	-4.56	0.39	0.12	0.44
	4652.158	21	1.00	-1.54	1		162.0	-4.46	0.39	0.09	0.34
	4708.040	186	3.15	+0.35	1		118.1	-4.60	0.40	0.11	0.47
	4718.429	186	3.18	+0.36	2		128.8	-4.56	0.40	0.11	0.43
	4756.113	145	3.09	+0.41	2		147.0	-4.51	0.40	0.10	0.39
	4922.267	143	3.09	+0.18	2		200.2	-4.39	0.43	0.08	0.24
	4936.334	166	3.10	-0.20	1		73.48	-4.83	0.44	0.10	0.42
	4954.811	166	3.11	-0.20	1		139.7	-4.55	0.44	0.10	0.35
	5206.039	7	0.94	-0.83	2	0.530	412.4	-4.10	0.48	0.06	0.14
	5247.564	18	0.96	-2.29	2		170.8	-4.45	0.49	0.06	0.21
	5296.686	18	0.98	-2.06	2		115.0	-4.66	0.50	0.07	0.35
	5297.360	94	2.89	+0.03	2		140.9	-4.58	0.50	0.07	0.29
	5298.269	18	0.98	-1.85	2	0.459	396.7	-4.13	0.50	0.06	0.13
	5329.12	94	2.90	-0.12	2		188.1	-4.45	0.50	0.06	0.21
	5345.807	18	1.00	-1.66	2	0.381	302.6	-4.25	0.51	0.05	0.13
	5348.319	18	1.00	-1.84	2		220.4	-4.38	0.51	0.05	0.15
	5409.791	18	1.03	-1.38	3		252.1	-4.33	0.52	0.05	0.14
Fe I-	4005.246	43	1.55	-1.32	2		319.0	-4.10	0.28	0.13	0.30
King	4045.815	43	1.48	-0.62	2	0.870	644.4	-3.80	0.29	0.13	0.27
	4063.597	43	1.55	-0.76	2		420.0	-3.99	0.29	0.13	0.27

TABLE II (Cont'd)

λ RMT	Multiplet (RMT)	χ_e	log gfλ	Number of Measures	R_c	W (MA)	log $\frac{W}{\lambda}$	B^0/B^1	Δ logη_o Scattering	Δ logη_o Absorption
4071.740	43	1.60	-0.81	2	0.831	471.0	-3.94	0.29	0.13	0.27
4143.871	43	1.55	-1.24	2		316.7	-4.12	0.30	0.12	0.27
4202.031	42	1.48	-1.43	4		316.8	-4.12	0.31	0.12	0.28
4206.702	3	0.05	-4.60	4		214.5	-4.29	0.31	0.12	0.29
4216.186	3	0.00	-4.05	4		241.7	-4.24	0.32	0.12	0.29
4250.790	42	1.55	-1.43	4		292.5	-4.16	0.32	0.12	0.26
4271.764	42	1.48	-0.98	2	0.805	483.0	-3.95	0.32	0.12	0.25
4291.466	3	0.05	-4.71	2		134.0	-4.51	0.33	0.14	0.51
4325.765	42	1.60	-0.78	3	0.822	588.4	-3.87	0.33	0.11	0.24
4337.049	41	1.55	-2.25	2		322.8*	-4.31	0.34	0.11	0.26
4375.932	2	0.00	-3.72	2		267.8	-4.21	0.34	0.11	0.26
4383.547	41	1.48	-0.60	2		133.6	-3.78	0.34	0.11	0.24
4389.244	2	0.05	-4.98	2		158.5	-4.54	0.34	0.14	0.55
4404.752	41	1.55	-0.88	2	0.794	593.8	-3.87	0.35	0.11	0.23
4415.125	41	1.60	-1.36	2	0.766	493.7	-3.95	0.35	0.11	0.24
4427.312	2	0.05	-3.72	2		311.1	-4.15	0.35	0.11	0.25
4461.654	2	0.09	-3.89	2		297.6	-4.18	0.36	0.10	0.25
4466.57	2	0.11	-4.86	2		263.0	-4.23	0.36	0.10	0.25
4489.741	2	0.12	-4.55	2		251.5	-4.25	0.36	0.10	0.25
5269.541	15	0.86	-2.05	2		446.4	-4.07	0.50	0.06	0.13
5328.042	15	0.91	-2.19	2	0.594	469.6	-4.05	0.51	0.06	0.08
5397.131	15	0.91	-2.66	2		387.2	-4.14	0.52	0.05	0.12
5405.778	15	0.99	-2.50	3		410.5	-4.12	0.52	0.05	0.12
5429.699	15	0.95	-2.56	3		438.6	-4.09	0.53	0.05	0.11
5434.527	15	1.01	-2.73	3		291.7	-4.27	0.53	0.05	0.12
5446.920	15	0.99	-2.63	3		452.0	-4.08	0.53	0.05	0.11
Fe I- 4219.364 Carter	800	3.56	-3.70	4		221.1	-4.28	0.32	0.12	0.29

TABLE II (Cont'd)

λ RMT	Multiplet (RMT)	χ_e	log $gf\lambda$	Number of Measures	R_c	W (MA)	log $\frac{W}{\lambda}$	B^0/B^1	$\Delta \log \eta_o$ Scattering	$\Delta \log \eta_o$ Absorption
4222.219	152	2.44	-4.99	4		195.7	-4.33	0.32	0.13	0.29
4227.42	693	3.32	-3.76	4	0.703	359.4	-4.07	0.32	0.12	0.25
4233.608	152	2.47	-4.66	4		239.0	-4.25	0.32	0.12	0.25
4235.942	152	2.41	-4.44	4	0.736	485.2	-3.94	0.32	0.12	0.25
4238.816	693	3.38	-4.06	4		231.5	-4.26	0.32	0.12	0.25
4247.432	693	3.35	-4.11	4		280.8	-4.18	0.32	0.12	0.26
4248.228	482	3.06	-4.44	4		251.4	-4.23	0.32	0.12	0.27
4250.125	152	2.46	-4.60	4		267.2	-4.20	0.32	0.12	0.27
4260.479	152	2.39	-4.19	2	0.744	414.9	-4.01	0.32	0.12	0.25
4271.159	152	2.44	-4.49	2		301.4	-4.15	0.32	0.12	0.25
4282.406	71	2.17	-4.74	2		241.1	-4.25	0.33	0.11	0.29
4430.618	68	2.21	-6.74	2		278.4	-4.20	0.35	0.11	0.22
4435.151	2	0.09	-8.32	2		236.7	-4.27	0.35	0.11	0.24
4442.343	68	2.19	-5.28	2		223.8	-4.30	0.35	0.11	0.24
4443.197	350	2.85	-3.99	2		219.5	-4.31	0.35	0.11	0.24
4447.722	68	2.21	-5.24	2		179.0	-4.40	0.35	0.14	0.29
4454.383	350	2.82	-4.69	2		197.2	-4.35	0.35	0.12	0.24
4494.568	68	2.19	-4.99	2		333.3	-4.13	0.36	0.10	0.22
4531.152	39	1.48	-6.09	1	0.533	374.0	-4.08	0.37	0.10	0.23
5191.460	383	3.03	-4.63	2		321.2	-4.21	0.48	0.06	0.15
5192.350	383	2.99	-4.46	2	0.467	354.8	-4.17	0.48	0.06	0.14
5194.943	36	1.55	-6.30	2		184.1	-4.45	0.48	0.08	0.21
5216.278	36	1.60	-6.29	2		307.8	-4.23	0.49	0.06	0.14
5232.946	383	2.93	-4.29	2	0.450	383.7	-4.13	0.49	0.06	0.13
5250.650	66	2.19	-6.23	2		308.0	-4.23	0.49	0.06	0.14
5266.562	383	2.99	-4.61	2		306.0	-4.24	0.49	0.06	0.14
5307.365	36	1.60	-7.11	2		152.5	-4.54	0.50	0.07	0.25
5324.185	553	3.20	-4.15	2		293.7	-4.26	0.50	0.06	0.10

IV. RESULTS FOR Ti I

Lines of only three multiplets of Ti I were able to be used. Only one line of the a^5P multiplet satisfied all the criteria for choosing lines to be measured. The a^5F multiplet had the most lines and the fit to the theoretical curve was based primarily on this multiplet. The determination of the vertical shift which gives log c/ν and the damping them came from the fit of the a^5F multiplet. However there was considerable scatter of this multiplet as well as the a^3F and the value of the damping constant, a, was approximated first by a rough calculation from the equation

$$a = \frac{1}{\Delta\nu_D} \cdot (\Gamma_r/4\pi + \Gamma_c/4\pi)$$

where $\Delta\nu_D$ is the Doppler width in units of frequency, Γ_r and Γ_c are the radiation and collisional damping, respectively. It is assumed van der Waals forces (collisions with neutral hydrogen atoms) are most important in the calculation of the collisonal damping constant.

For M-E and S-S scattering theoretical curves for log a = -1.0, -1.4, -1.8, and -2.0, were available and the best fit was found from the a^5F multiplet to be at log a = -1.4. The possibilities in the S-S absorption curves were log a = -1.0, -1.05, -2.0. The best fit here was for log a = -1.5. Only two values of log a were available for the M-E absorption curves. They were for log a = -1.0 and -3.0. The best fit for this model was found to be for the log a = -1.0 curve.

The observed curves of growth were made by plotting log W/λ as the ordinate and log $gf\lambda_{rel}$ as the abscissa for each observed line. It will be shown that the temperature is found from a linear relationship between the horizontal shift for each multiplet and the excitation potential and thus that the relative f-values may be used in the determination of the excitation temperature.

It has been mentioned that corrections must be made in the observed curves due to limb darkening. These limb darkening shifts $\Delta \log \eta_o$ are listed in Table II and have been added to log $gf\lambda_{rel}$ for the M-E scattering and M-E absorption curves. The corresponding corrections, $\Delta \log \tau_o$, for the S-S curves were negligible and no corrections were made for these plots.

The theoretical curves used in this study were for $B^o/B^{\frac{1}{4}} = 2/3$ for the M-E models and $I^o/I^{\frac{1}{4}} = 2/3$ for the S-S models. The corrections mentioned above were to reduce all values of $B^o/B^{\frac{1}{4}}$ to this single value.

For all but the S-S pure absorption curves the ordinate of the theoretical curves is log $\frac{W}{b}$ where $b = \frac{\lambda v}{c}$. Then log $\frac{W}{b}$ may be written as log $\frac{W}{\lambda}$ + log c/v. Thus log c/v is found directly from the vertical shift except in the case of S-S pure absorption. For this model log $\frac{W}{2R_c b}$ is the ordinate. We may write this as

$$\log \frac{W}{\lambda} + \log c/v - \log 2 - \log R_c.$$

Then the vertical shift here is

$$\Delta \log \frac{W}{2R_c b} = \log c/v - \log 2 - \log R_c$$

and thus,

$$\log c/v = \Delta \log \frac{W}{2R_c b} + \log 2 + \log R_c.$$

The values of R_c, the central intensity, were found for the strongest

lines as listed in Table II. These values were weighted according to the number of observations on each line and a value of $\log R_c = -0.286$ was used for Ti I. The horizontal shifts were used in finding the abundances. The procedure employed will be described later.

The abscissa of the M-E theoretical curves is $\log \eta_o$. This may be written

$$(9) \quad \log \eta_o = \log N/\rho\bar{R} + \log \frac{\pi^{1/2} e^2}{mc^2} - \log u + \log c/v + \log gf\lambda - \theta\chi_e$$

All the quantities are as defined previously. However it should be noted that f is the <u>absolute</u> <u>f-value</u> here. More shall be said about this in the discussion of the abundance determination.

If we denote the horizontal shift by $\Delta \log X$, we may write, from (9),

$$(10) \quad \Delta \log X = \log \eta_0 - (\log gf\lambda_{rel} + \Delta \log \eta_o).$$

Since only the horizontal shift and the excitation potential depend upon the multiplet we may write (10) as

$$(11) \quad \Delta \log X = \text{constant} - \theta \chi_e.$$

A plot of this relation is made for each multiplet. A weight was assigned to each shift depending upon the number of lines measured in each multiplet and how well it fitted the curve of growth. Those terms having only one measurement or obviously far out of line with the others were given zero weight. A least squares solution gave the value of θ and hence the slope of the line through the plotted points resulting from (11). Figure 4 shows the results of the solutions for each model.

Since $\theta = \frac{5040}{T}$, the excitation temperatures were found for each model from this relation. The probable errors in the temperature were taken from the probable error in the least squares solution for θ.

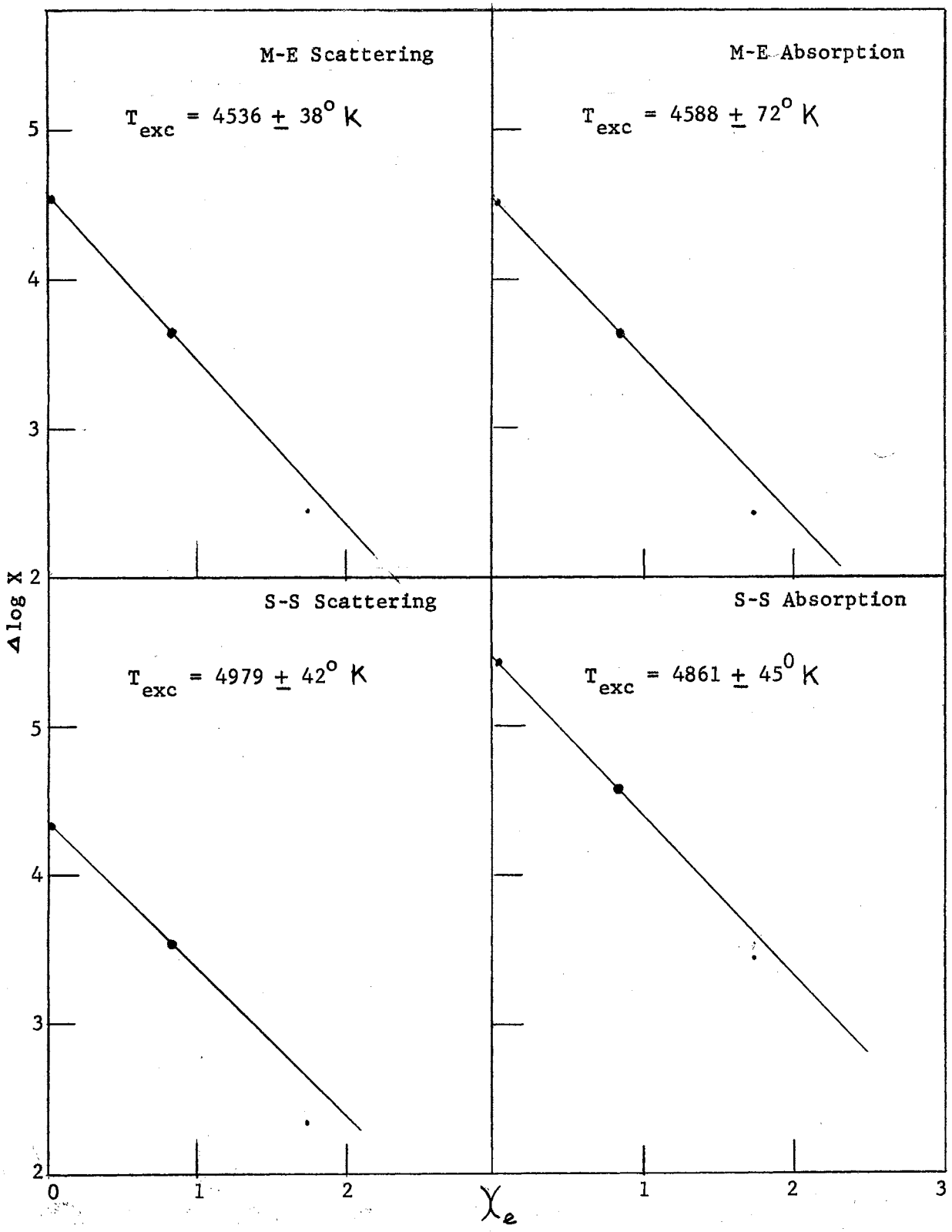

Figure 4. Excitation Temperatures Derived from Ti I Lines

For S-S scattering curves the abscissa is $\log \tau_o$. Then

(12) $\log \tau_o = \log NH + \log \frac{\pi^{1/2} e^2}{mc^2} - \log u + \log gf\lambda + \log c/v - \theta \chi_e$,

where the remarks made concerning (9) are applicable here also. As in the M-E model equation (11) holds and the temperature may be found after plotting $\Delta \log X$ versus $\theta \chi_e$.

For S-S absorption, the curves of Munger (1956) were available. Changing his notation to that of the other theoretical curves we have for the abscissa $\log \tau_o/R_c$. Then

(13) $\log \tau_o/R_c = \log NH + \log \frac{\pi^{1/2} e^2}{mc^2} = \log u + \log gf\lambda + \log c/v - \theta \chi_e - \log R_c$.

Again we plot $\Delta \log X$ versus $\theta \chi_e$ and find the excitation temperature.

Table III list all four results. The excitation temperatures with their probable errors are given at the bottom of the table.

To determine the abundances a few changes must be made. Now one plots for each multiplet $\log W/\lambda$ versus $\log gf_{rel}\lambda - \theta \chi_e$ where θ has been determined in the least squares solution. Also it is necessary to use the absolute f-values rather than the relative. Let us define

$$gf = gf_{abs} = K gf_{rel} \text{ or}$$

$$\log gf = \log gf_{rel} + \log K.$$

Denote $\log K$ by $\Delta \log gf$. Then for the M-E models equation (9) becomes

(14) $\log \eta_o = \log N/\rho\bar{K} + \log C - \log u + \log c/v + \log gf_{rel}\lambda + \Delta \log gf - \theta \chi_e$

Here $\log C = \log \frac{\pi^{1/2} e^2}{mc^2} = -12.30$.

For the multiplet plots of $\log W/\lambda$ versus $\log gf_{rel}\lambda - \theta \chi_e + \Delta \log \eta_o$ a fit is obtained to the same curve used in the temperature determination using the same vertical shift. The horizontal shift is then

(15) shift = $\log N/\rho\bar{K} + \log C - \log u + \log c/v + \Delta \log gf$

TABLE III

CURVE OF GROWTH DATA DERIVED FROM Ti I LINES

				M-E Model		S-S Model	
				Scattering	Absorption	Scattering	Absorption
log c/v				5.15	5.20	5.20	5.22
log a				-1.4	-1.0	-1.4	-1.5
Term	χ_e	No. of Lines	Weight	Δ log X	Δ log X	Δ log X	Δ log X
a^3F	0.02	6	1	4.55	4.53	4.35	5.43
a^5F	0.83	9	2	3.65	3.64	3.53	4.59
a^5P	1.73	1	0	2.45	2.45	2.32	3.45
Excitation Temperature (^oK)				4536 $\pm$ 38	4588 $\pm$ 72	4979 $\pm$ 42	4861 $\pm$ 45

Then,

(16) $\log N/\rho\bar{K} = \text{shift} - \log C + \log U - \log c/\nu - \Delta \log gf.$

The shift obtained here is in reality merely $\Delta \log X$ found in the temperature determination with the factor $\theta \chi_e$ added in each case. Then the shift is found for each multiplet and a weighted value is determined using the same weights as in the temperature determination.

The values of the partition function, U, were determined from the values given by Claas (1951) with extrapolations made where necessary.

For Ti I the value of $\Delta \log gf$ was found to be -3.30. This value is based upon the absolute f-values of Ti I as determined by Allen (1955).

Pertinent abundance data for Ti I is given in Table IV. Some of the data from Table III are repeated for convenience in interpretation.

For S-S scattering abundance determination, one obtains an equation analogous to equation (16). This is

(17) $\log NH = \text{shift} - \log C + \log U - \log c/\nu - \Delta \log gf.$

Due to the difference in abcissas one obtains for S-S absorption.

(18) $\log NH = \text{shift} - \log C + \log U - \log c/\nu - \Delta \log gf + \log R_c.$

The abundances shown at the bottom of Table IV were determined from equations (16), (17), and (18).

The four resultant curves of growth for Ti I are shown in Figures 5, 6, 7, and 8. The ordinates in each case are $\log W/\lambda$. The zero points for the theoretical curves are shown by long strokes. For the M-E models the abscissas are $\log \eta_o$. For S-S scattering it is $\log \tau_o$ and for S-S absorption $\log \tau_o/R_c$.

The abundances determined are for the neutral atoms only. To find the abundance contribution of the ionized atoms Saha's equation (8) is

TABLE IV

CURVE OF GROWTH ABUNDANCE DATA FOR Ti I

			M-E Model		S-S Model	
			Scattering	Absorption	Scattering	Absorption
log a			-1.4	-1.0	-1.4	-1.5
θ			1.111	1.099	1.012	1.037
log u			1.45	1.45	1.47	1.47
Term	χ_e	Weight	Shift	Shift	Shift	Shift
a^3F	0.02	1	4.57	4.55	4.37	5.45
a^5F	0.83	2	4.57	4.55	4.37	5.45
a^5P	1.73	0	4.37	4.35	4.07	5.24
Weighted Shift			4.57	4.55	4.37	5.45
Abundance		log $N/\rho\bar{K}$	16.49	16.42		
		log NH			16.24	17.01

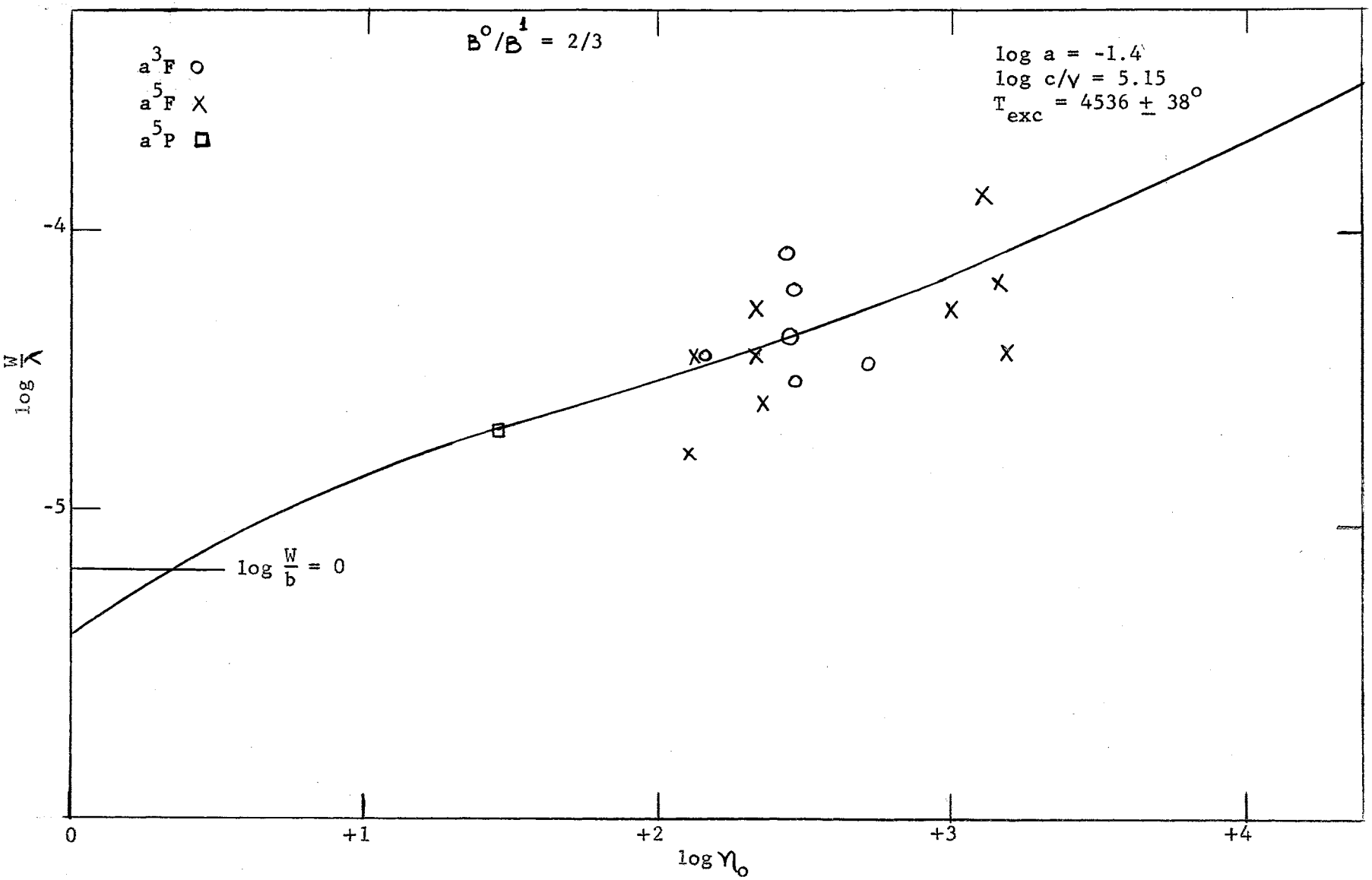

Figure 5. Milne-Eddington Pure Scattering Curve of Growth for Ti I

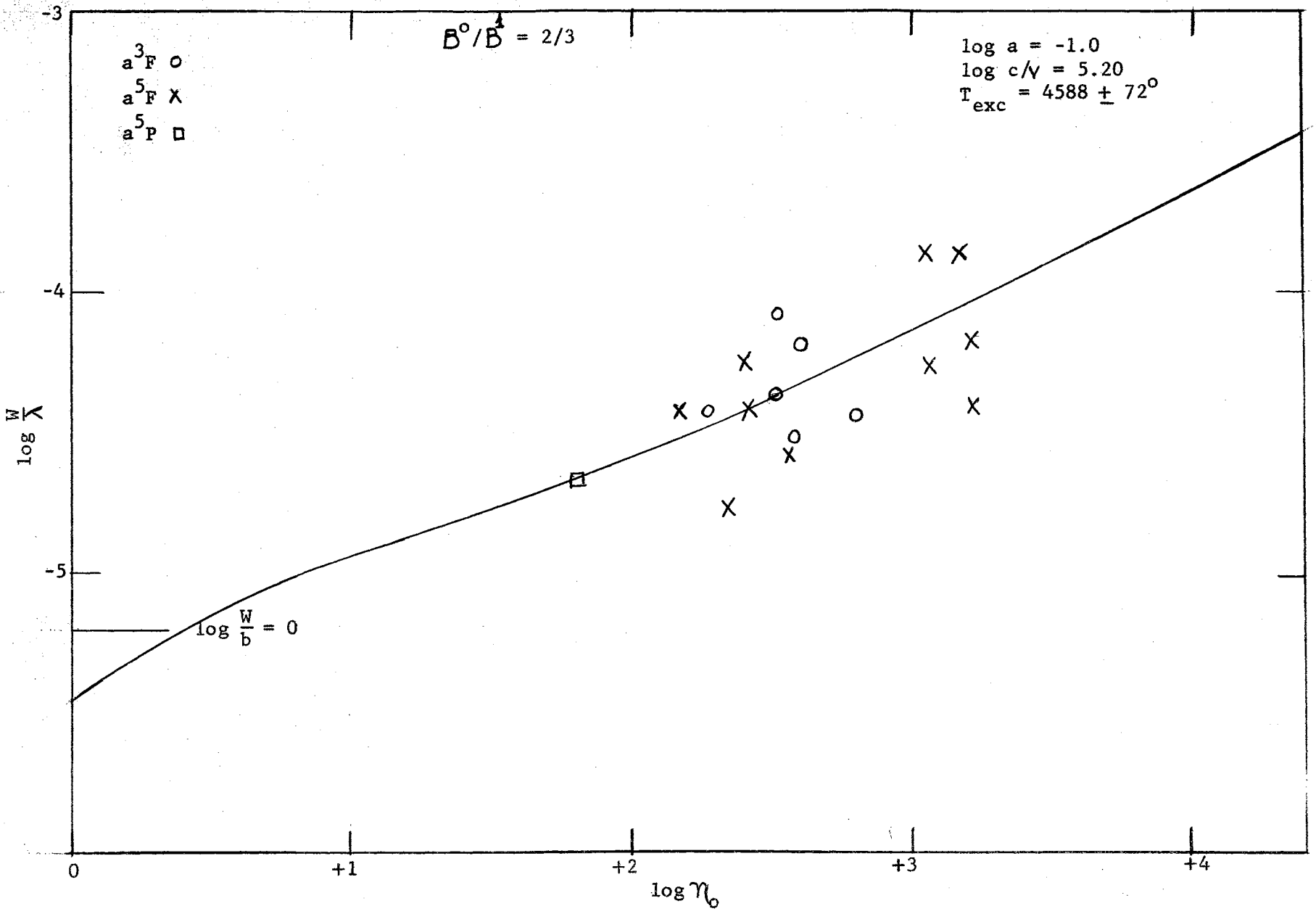

Figure 6. Milne-Eddington Pure Absorption Curve of Growth for Ti I

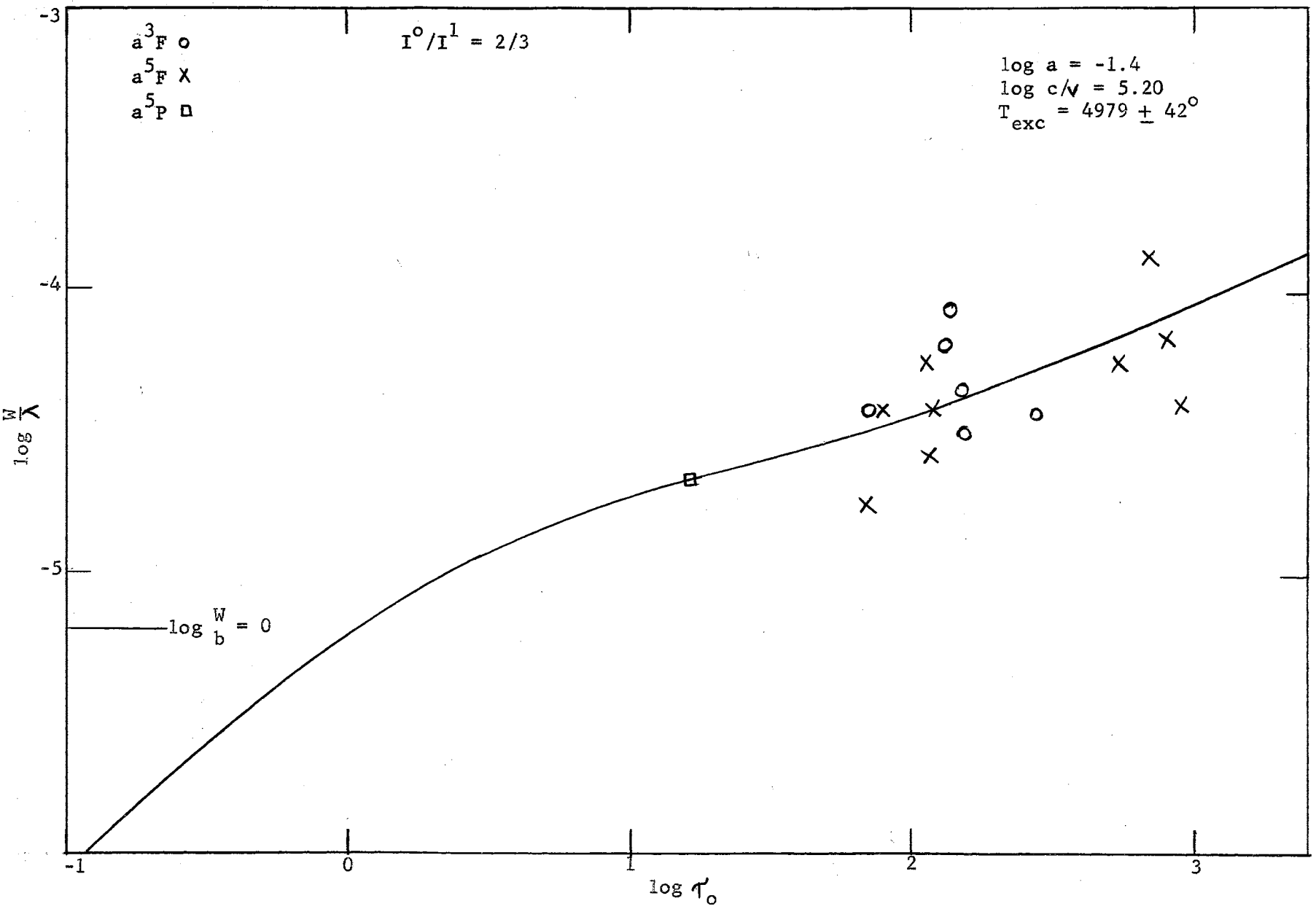

Figure 7. Schuster-Schwarzschild Pure Scattering Curve of Growth for Ti I

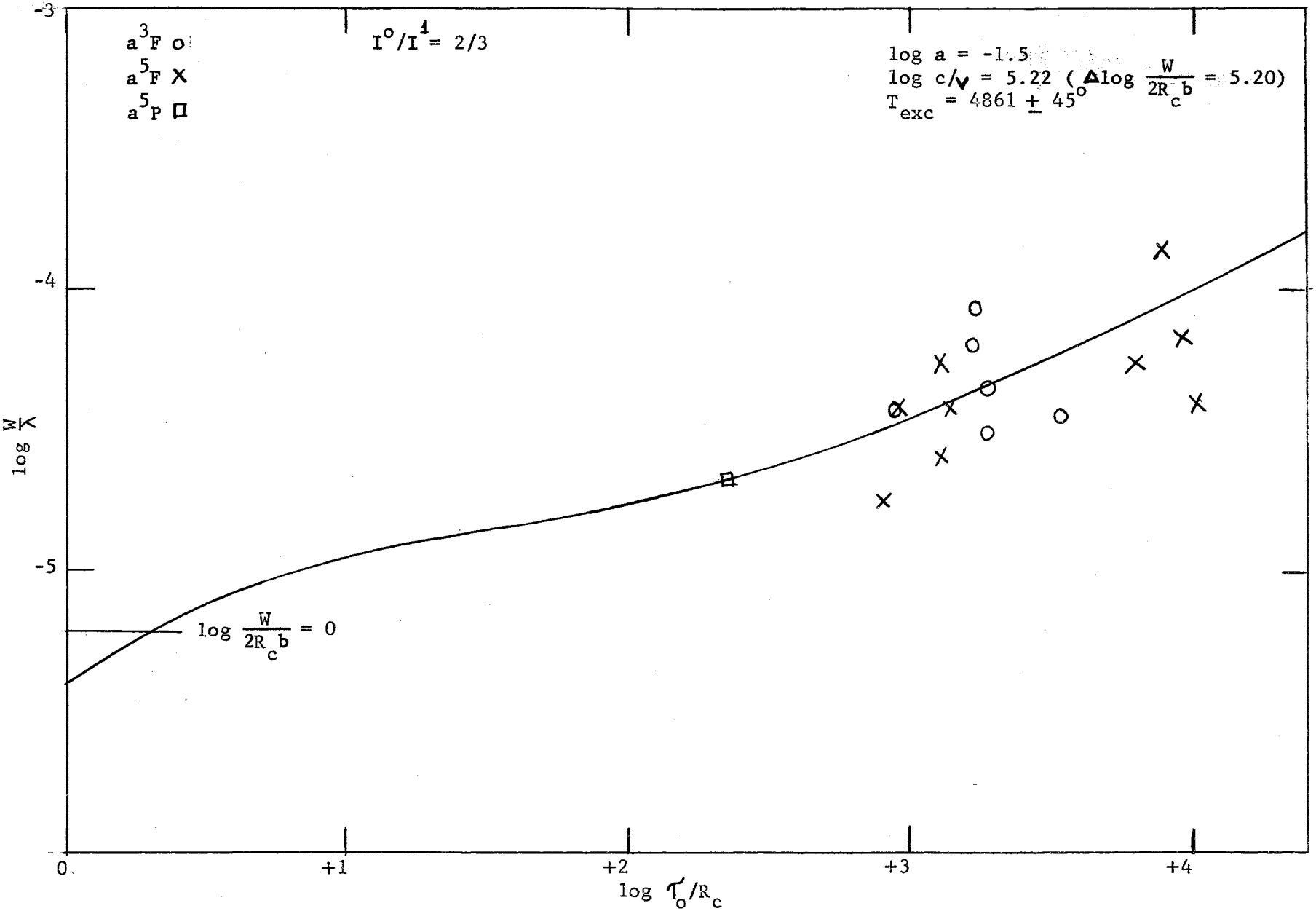

Figure 8. Schuster-Schwarzschild Pure Absorption Curve of Growth for Ti I

used. Here log p_e was taken as -0.4, χ_i was taken from the Revised Multiplet Table, T was assumed to be approximately equal to the effective temperature and this was also used in computing θ, and as before the partition functions are from Claas (1956).

These values of T and p_e were used since they are what the values at optical depth 0.6 in the atmosphere of this star would likely be, and this is a representative depth for line formation.

The quantity actually determined is $\log \frac{(NH)_1}{(NH)_o}$, or $\log \frac{(N/\rho\bar{K})_1}{(N/\rho\bar{K})_2}$. Since second ionizations are negligible, the total abundance is given by

$$\log (NH)_T = \log \left[(NH)_o + (NH)_1 \right] = \log \left\{ (NH)_o \left[1 + \frac{(NH)_1}{(NH)_o} \right] \right\}$$
$$= \log (NH)_o + \Delta \log NH.$$

For the M-E models, one substitutes $N/\rho\bar{K}$ for NH. The value of $\Delta \log NH$ or $\Delta \log N/\rho\bar{K}$ for Ti I was found to be 2.31.

V. RESULTS FOR Cr I

The procedures here were the same as outlined in the previous section. Excitation temperatures and other data found in the curve fitting processes are listed in Table VI.

The value of log a used in each case and the vertical shift, log c/y, were determined from the fit of the a^5D multiplet plot.

Figure 9 gives the plots of Δlog X versus χ_e and the straight line resulting from the least squares solution for each model.

The value of Δlog gf was taken as -3.42 for Cr I. This value is based upon the absolute f-values of Bell, et al (1958). Abundance data for Cr I are shown in Table VI. The value of log R_c was found to be -0.253.

The curves of growth obtained for Cr I are shown in Figures 10, 11, 12, and 13.

The value of Δlog NH or Δlog $N/\rho\bar{K}$ for Cr I was found to be 1.94.

TABLE V

CURVE OF GROWTH DATA DERIVED FROM Cr I LINES

				M-E Model		S-S Model	
				Scattering	Absorption	Scattering	Absorption
log c/v				5.17	5.05	5.23	5.10
log a				-1.4	-1.0	-1.4	-1.5
Term	χ_e	Measures	Weight	Δ log X	Δ log X	Δ log X	Δ log X
a^7S	0.00	3	0	4.49	3.99	4.47	4.95
a^5S	0.94	2	1	4.05	3.59	3.96	4.47
a^5D	0.99	15	3	4.15	3.67	4.09	4.54
a^5P	2.70	2	0	3.05	2.41	2.96	3.59
z^7P^o	2.89	3	1	2.03	1.55	1.73	2.31
a^3H	2.98	2	0	2.33	1.77	2.29	2.77
a^3G	3.09	2	1	1.85	1.40	1.78	2.26
a^3F	3.10	2	0	1.60	1.15	1.08	1.46
z^7F^o	3.16	2	1	1.36	0.82	1.30	1.75
Excitation Temperature (^oK)				4339 $\pm$ 197	4317 $\pm$ 221	4212 $\pm$ 180	4238 $\pm$ 185

TABLE VI

CURVE OF GROWTH ABUNDANCE DATA FOR Cr I

			M-E Model		S-S Model	
			Scattering	Absorption	Scattering	Absorption
log a			-1.4	-1.0	-1.4	-1.5
θ			1.16	1.17	1.20	1.19
log u			0.95	0.95	0.93	0.94
Term	χ_e	Weight	Shift	Shift	Shift	Shift
a^7S	0.00	0	4.49	3.99	4.47	4.95
a^5S	0.94	1	5.14	4.69	5.09	5.59
a^5D	0.99	3	5.30	4.83	5.28	5.72
a^5P	2.70	0	6.18	5.57	6.20	6.80
z^7P^o	2.89	1	5.38	4.93	5.20	5.75
a^3H	2.98	0	5.79	5.26	5.87	6.32
a^3G	3.09	1	5.43	5.02	5.49	5.94

TABLE VI (Cont'd)

Term	χ_e	Weight	Shift	Shift	Shift	Shift
a^3F	3.10	0	5.20	4.78	4.80	5.15
a^7F^o	3.16	1	5.03	4.52	5.09	5.51
Weighted Shift			5.27	4.81	5.24	5.71
Abundance		log $N/\rho\bar{K}$	16.77	16.42		
		log NH			16.66	16.92

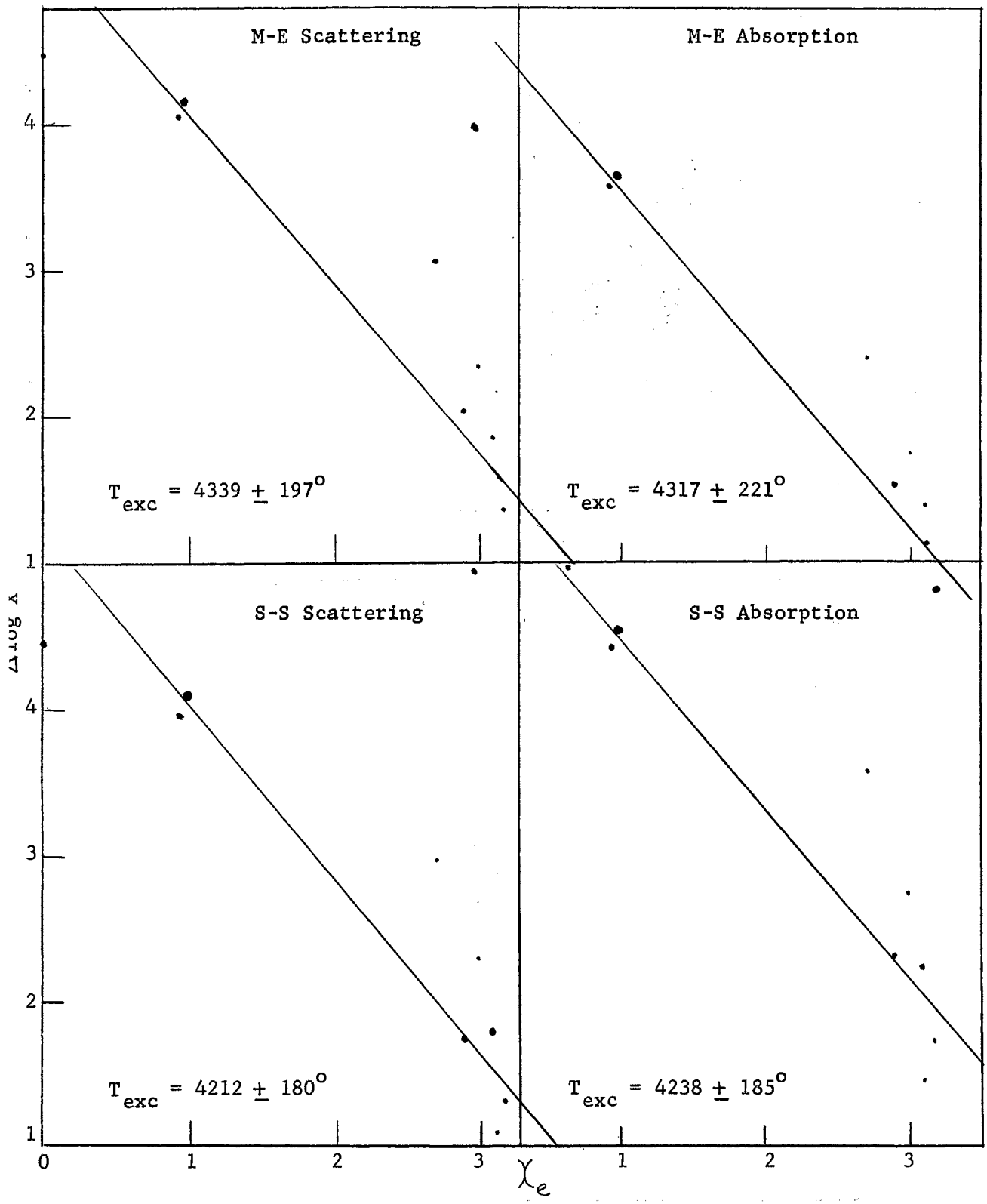

Figure 9. Excitation Temperatures Derived from Cr I Lines

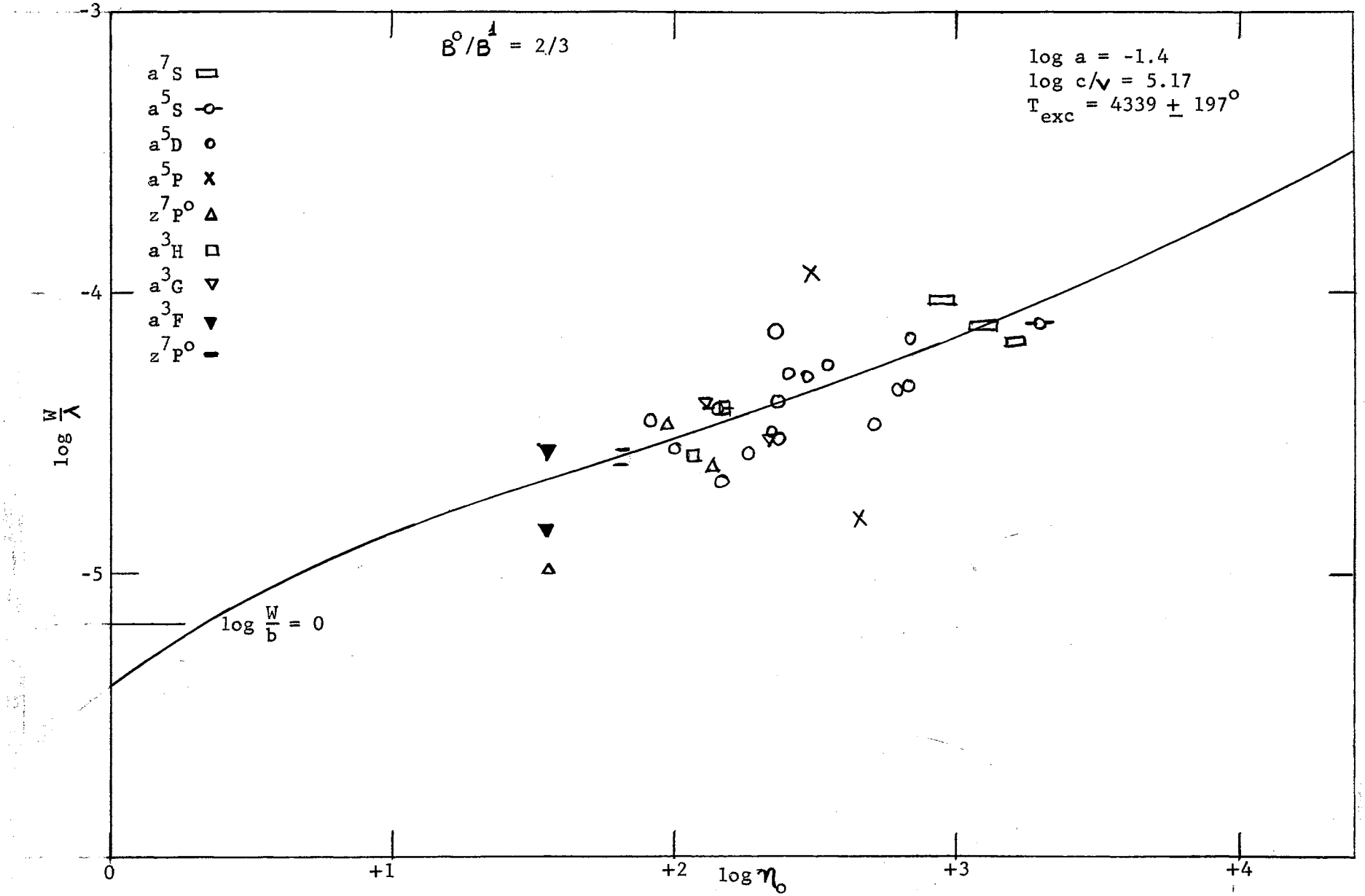

Figure 10. Milne-Eddington Pure Scattering Curve of Growth for Cr I

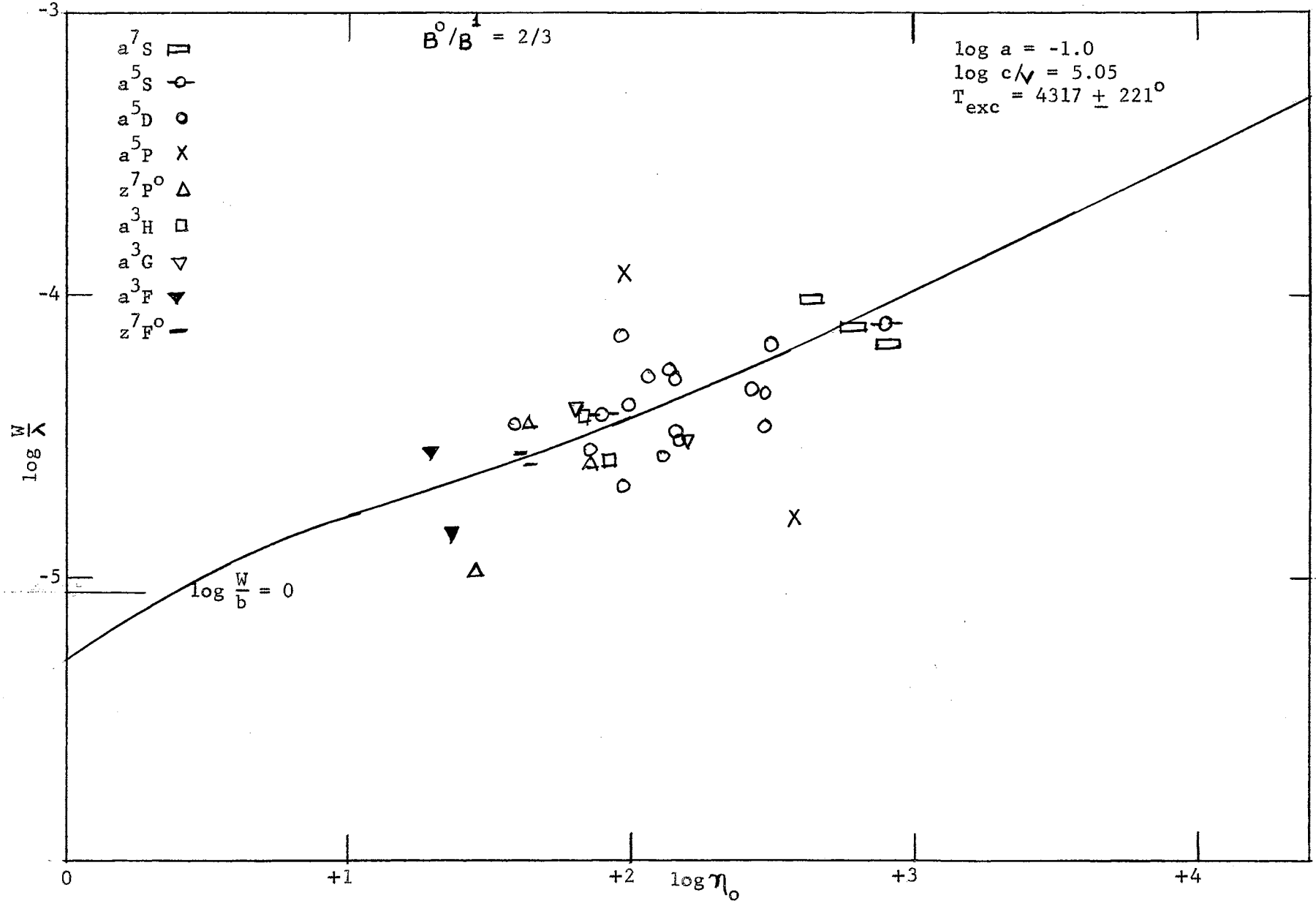

Figure 11. Milne-Eddington Pure Absorption Curve of Growth for Cr I

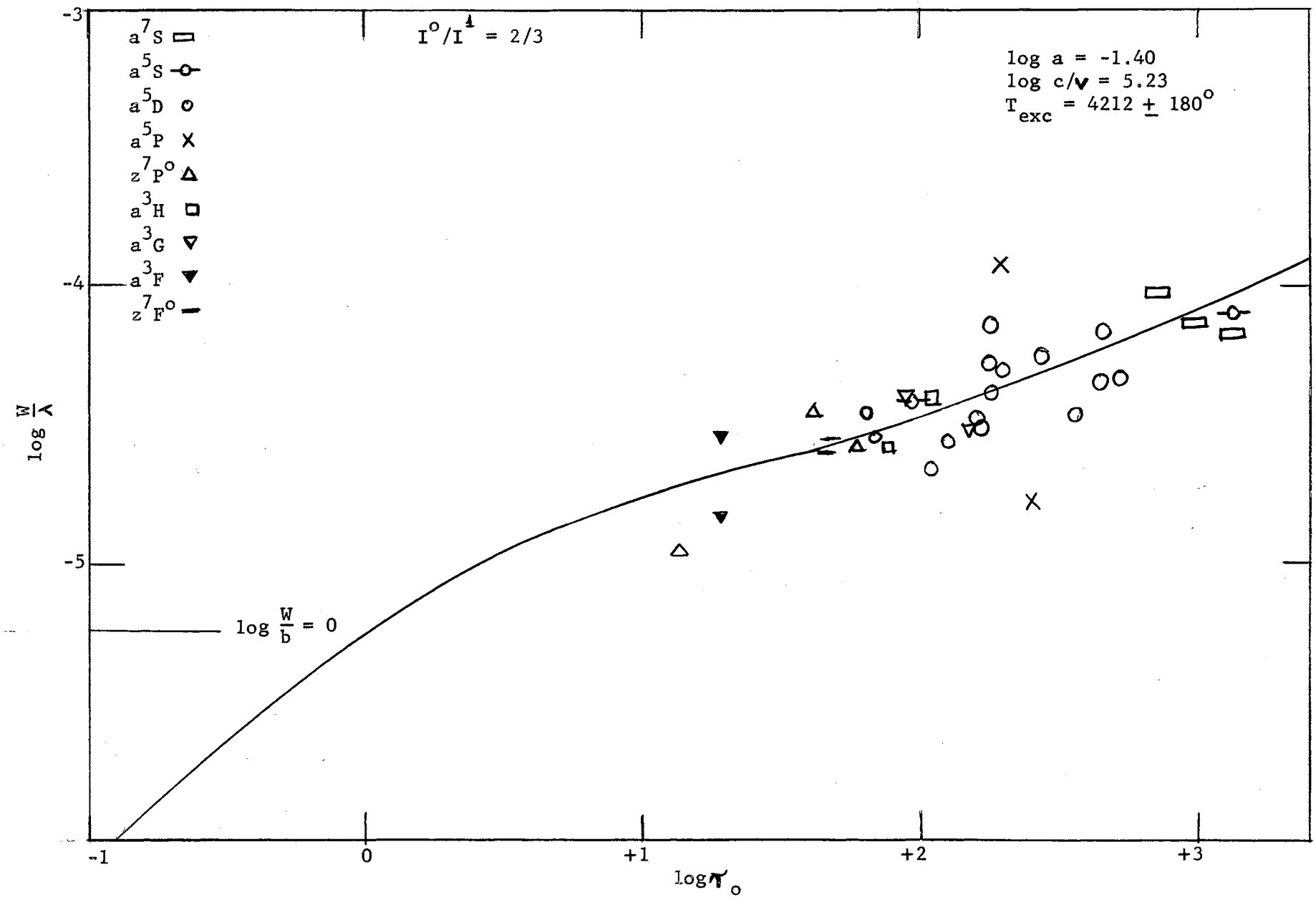

Figure 12. Schuster-Schwarzschild Pure Scattering Curve of Growth for Cr I

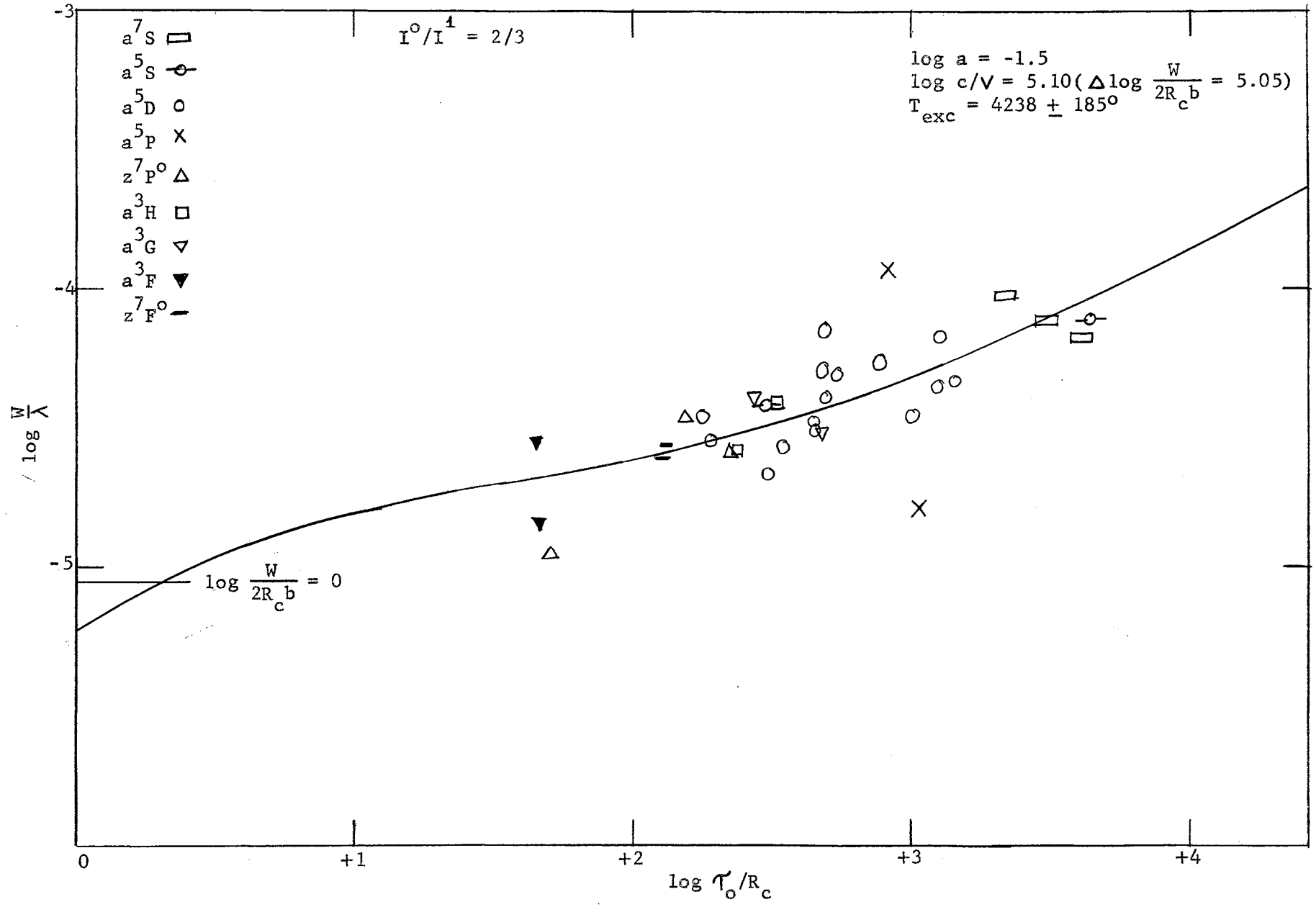

Figure 13. Schuster-Schwarzschild Pure Absorption Curve of Growth for Cr I

VI. RESULTS FOR Fe I

Because of the different f-values used the results for Fe I are in two parts.

Fe I-King.--A value of -3.24 was taken as the value of $\Delta \log gf$, again given by Bell, et al (1958). The value of $\log R_c$ was -0.105. Both the a^5D and a^3F multiplets were used in determining log a and log c/v.

Data pertinent to the temperature determination is listed in Table VII. Figure 14 shows the lines resulting from the least squares solution for θ.

Abundance data are found in Table VIII and the observed curves of growth are shown by Figures 15, 16, 17, and 18.

Fe I-Carter.--Absolute f-values were used here and hence no correction factor was needed. Log R_c was taken as -0.193. Several multiplets were used here in the determination of log a.

The excitation temperature and data used in its determination are shown in Table IX. Lines and plots used in the determination of θ are shown in Figure 19. Abundance data is given in Table X. Curves of growth for these lines appear on Figures 20, 21, 22, and 23.

Fe I-King and Carter.--As a point of interest combined Fe I curves of growth, based on both King's and Carter's f-values, are shown in Figures 24, 25, 26, and 27. The value of $\Delta \log NH$ or $\Delta \log N/\rho\bar{K}$ does not depend on the f-value and for Fe I this is 1.19.

TABLE VII

CURVE OF GROWTH DATA DERIVED FROM Fe I-KING LINES

				M-E Model		S-S Model	
				Scattering	Absorption	Scattering	Absorption
log c/v				5.09	4.95	5.05	5.07
log a				-1.8	-1.0	-1.8	-1.5
Term	χ_e	Measures	Weight	Δ log X	Δ log X	Δ log X	Δ log X
a^5D	0.06	9	2	6.88	6.01	6.48	6.75
a^5F	0.95	7	1	5.66	4.87	5.28	5.48
a^3F	1.54	13	2	4.58	3.65	4.29	4.39
Excitation Temperature (^oK)				3256 $\pm$ 91	3180 $\pm$ 94	3476 $\pm$ 375	3171 $\pm$ 62

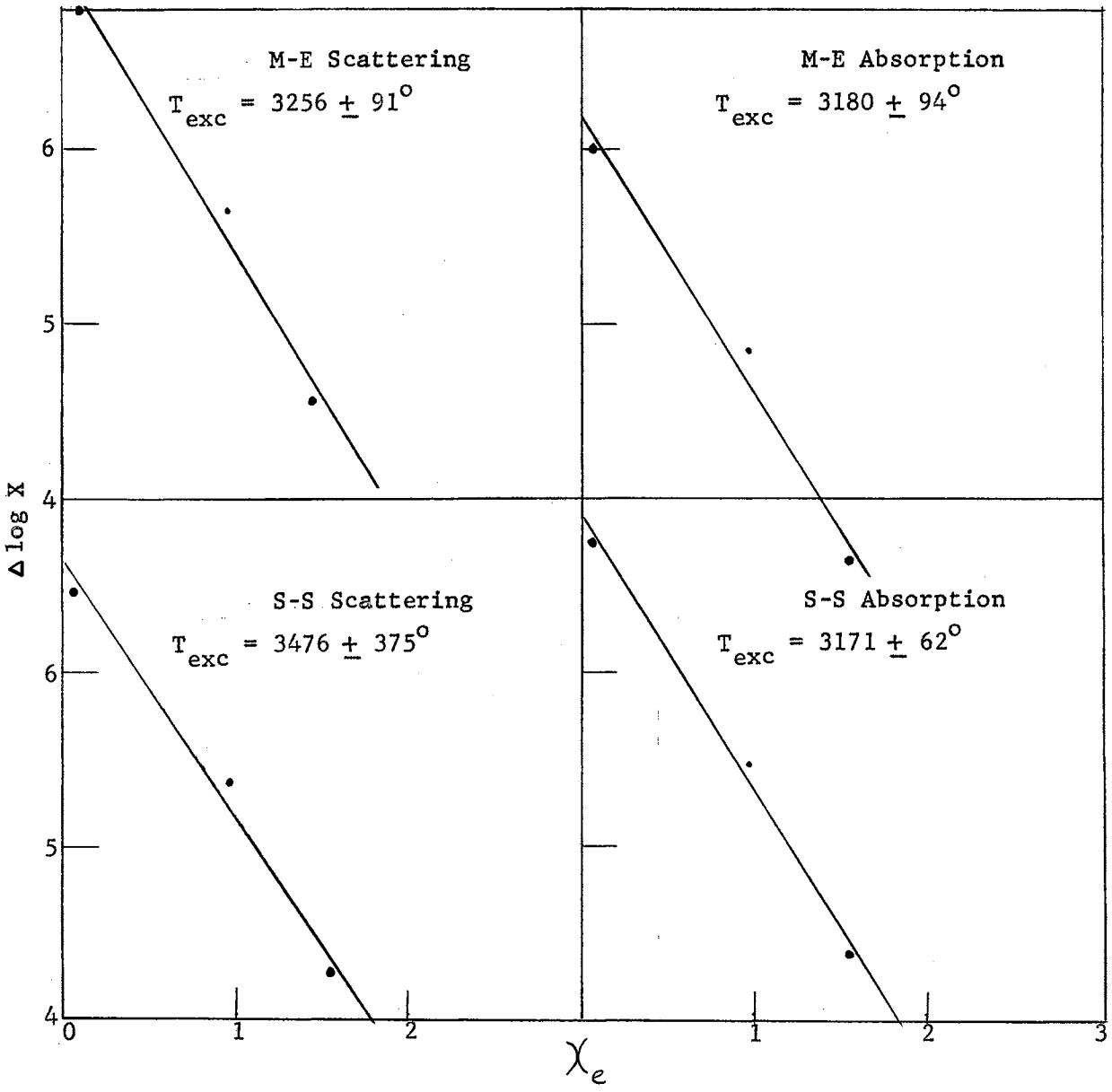

Figure 14. Excitation Temperatures Derived from Fe I-King Lines

TABLE VIII

CURVE OF GROWTH ABUNDANCE DATA FOR FeI-KING

			M-E Model		S-S Model	
			Scattering	Absorption	Scattering	Absorption
log a			-1.8	-1.0	-1.8	-1.5
θ			1.55	1.59	1.47	1.59
log u			1.37	1.37	1.38	1.37
Term	χ_e	Weight	Shift	Shift	Shift	Shift
a^5D	0.06	2	6.97	1.11	6.57	6.85
a^5F	0.95	1	7.13	6.38	6.68	6.99
a^3F	1.54	2	6.97	6.10	6.54	6.84
Weighted Shift			7.00	6.16	6.58	6.87
Abundance		log $N/\rho\bar{\kappa}$	18.82	18.12		
		log NH			18.45	18.61

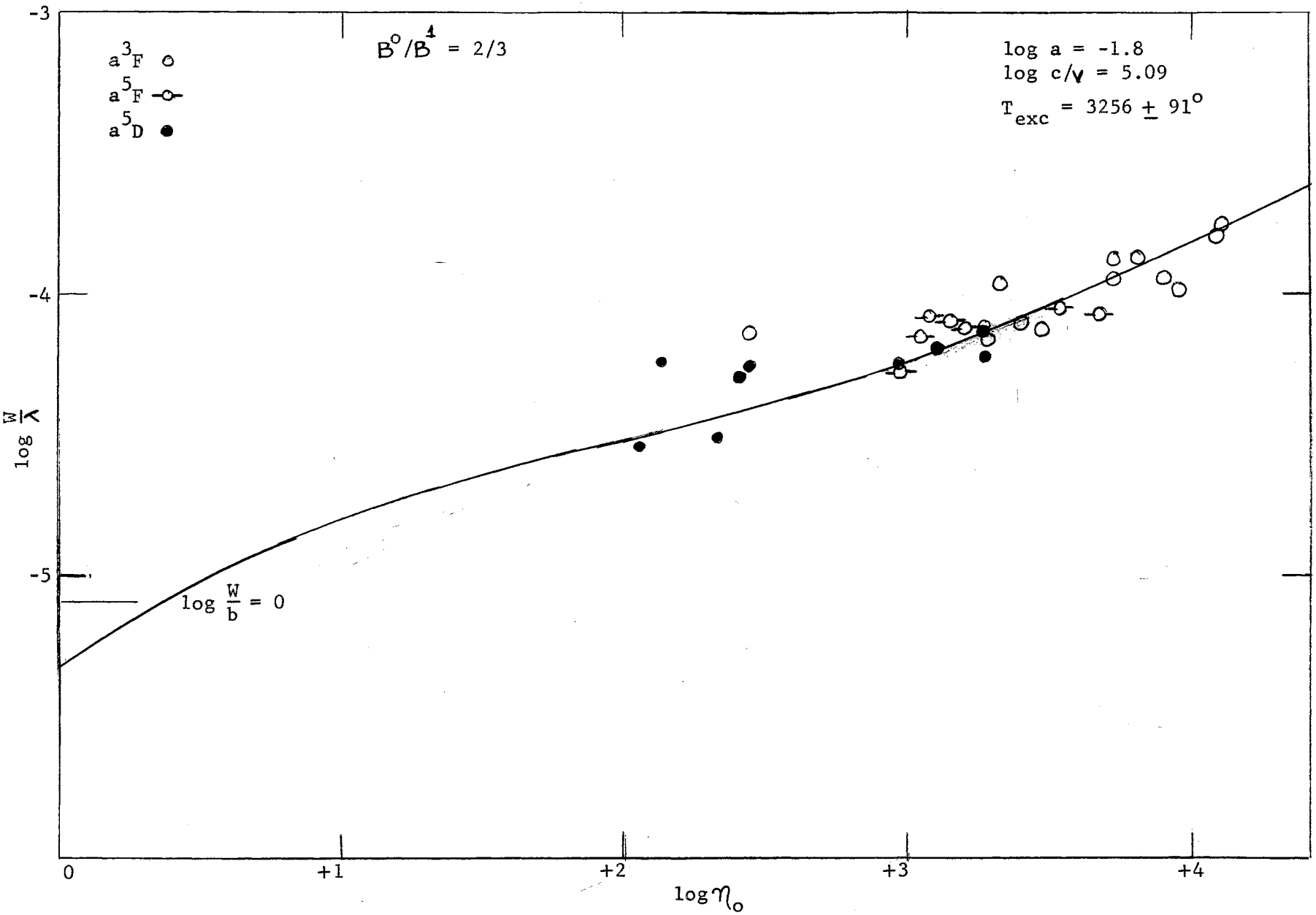

Figure 15. Milne-Eddington Pure Scattering Curve of Growth for Fe I-King

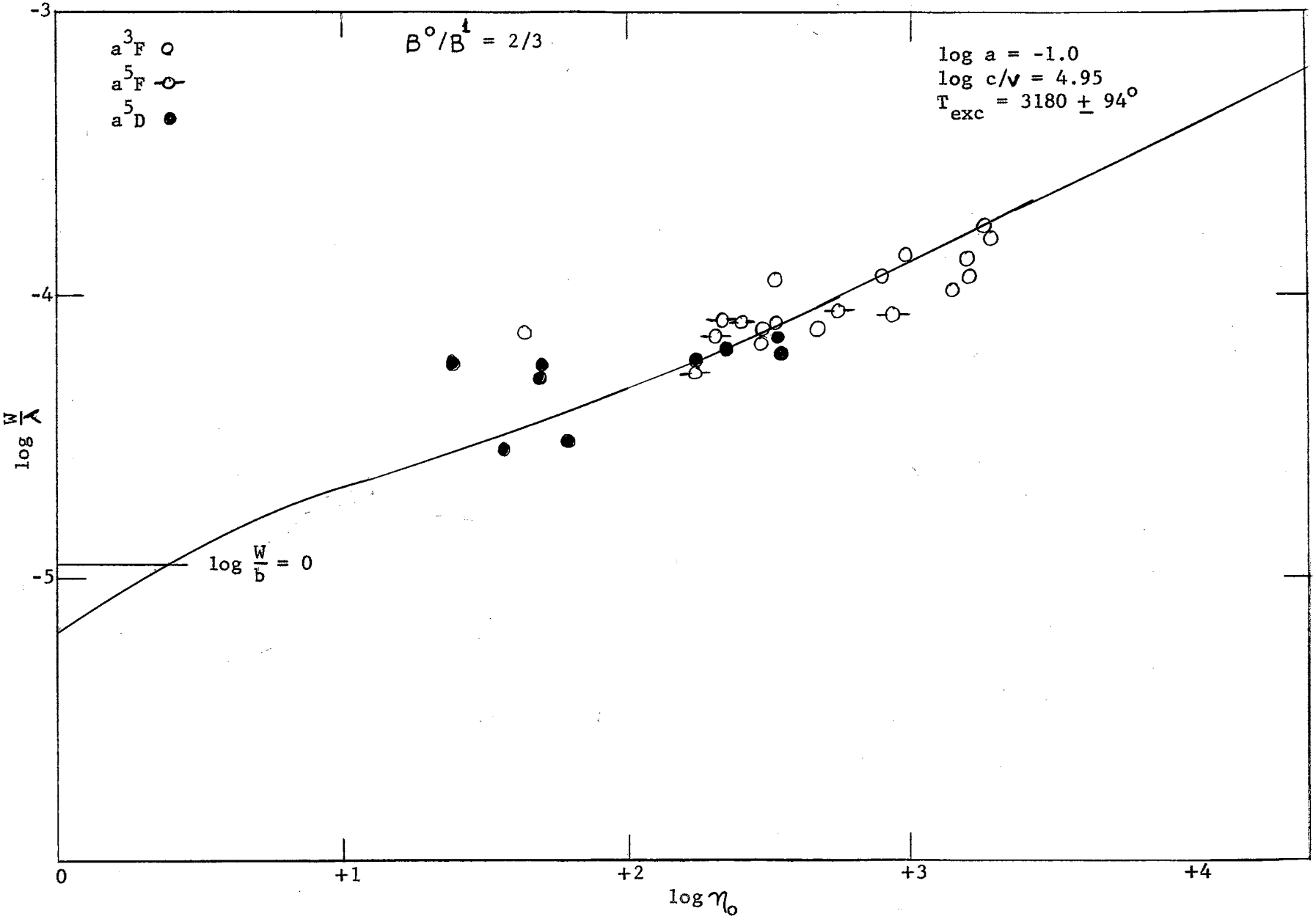

Figure 16. Milne-Eddington Pure Absorption Curveof Growth for Fe I-King

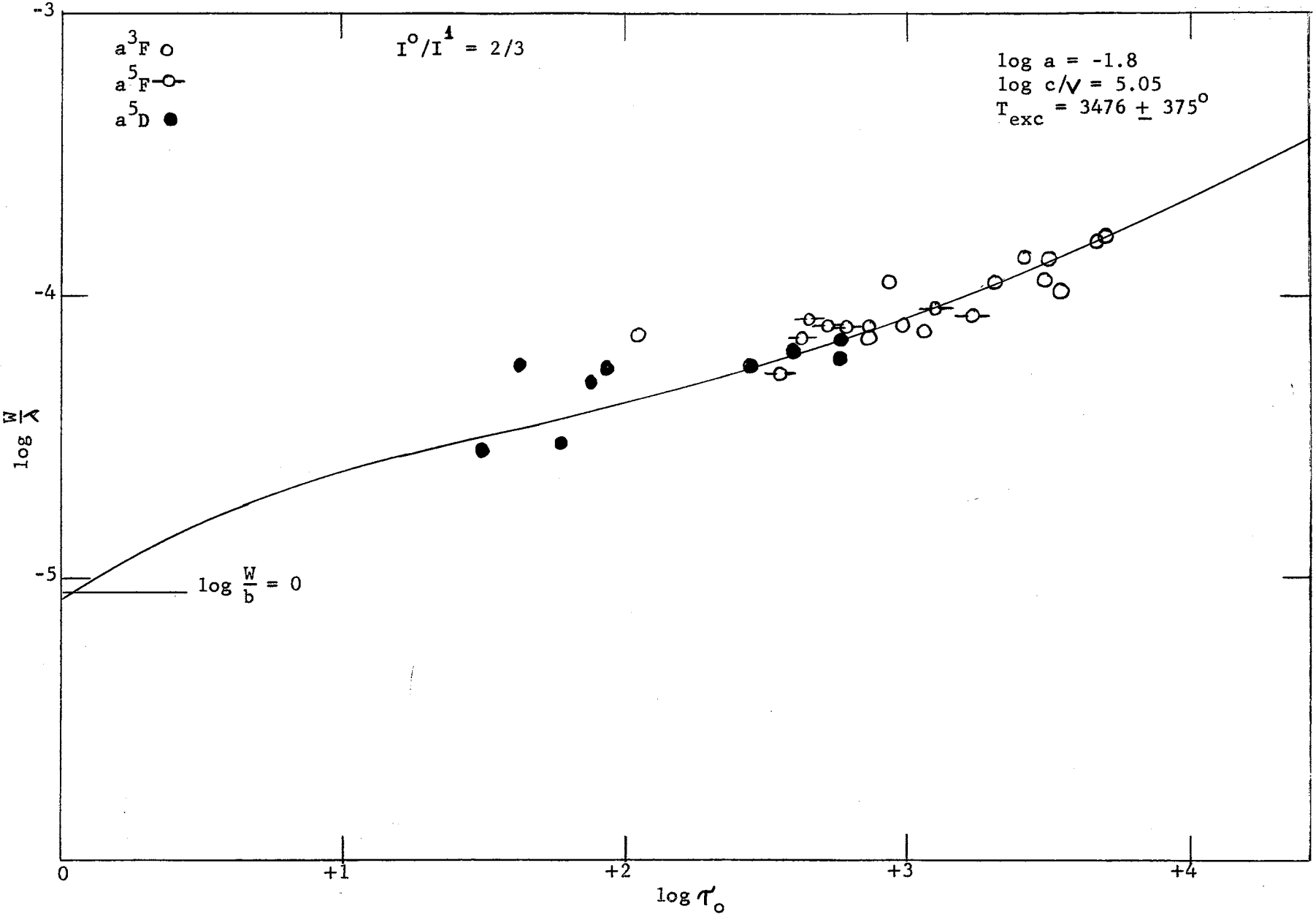

Figure 17. Schuster-Schwarzschile Pure Scattering Curve of Growth for Fe I-King

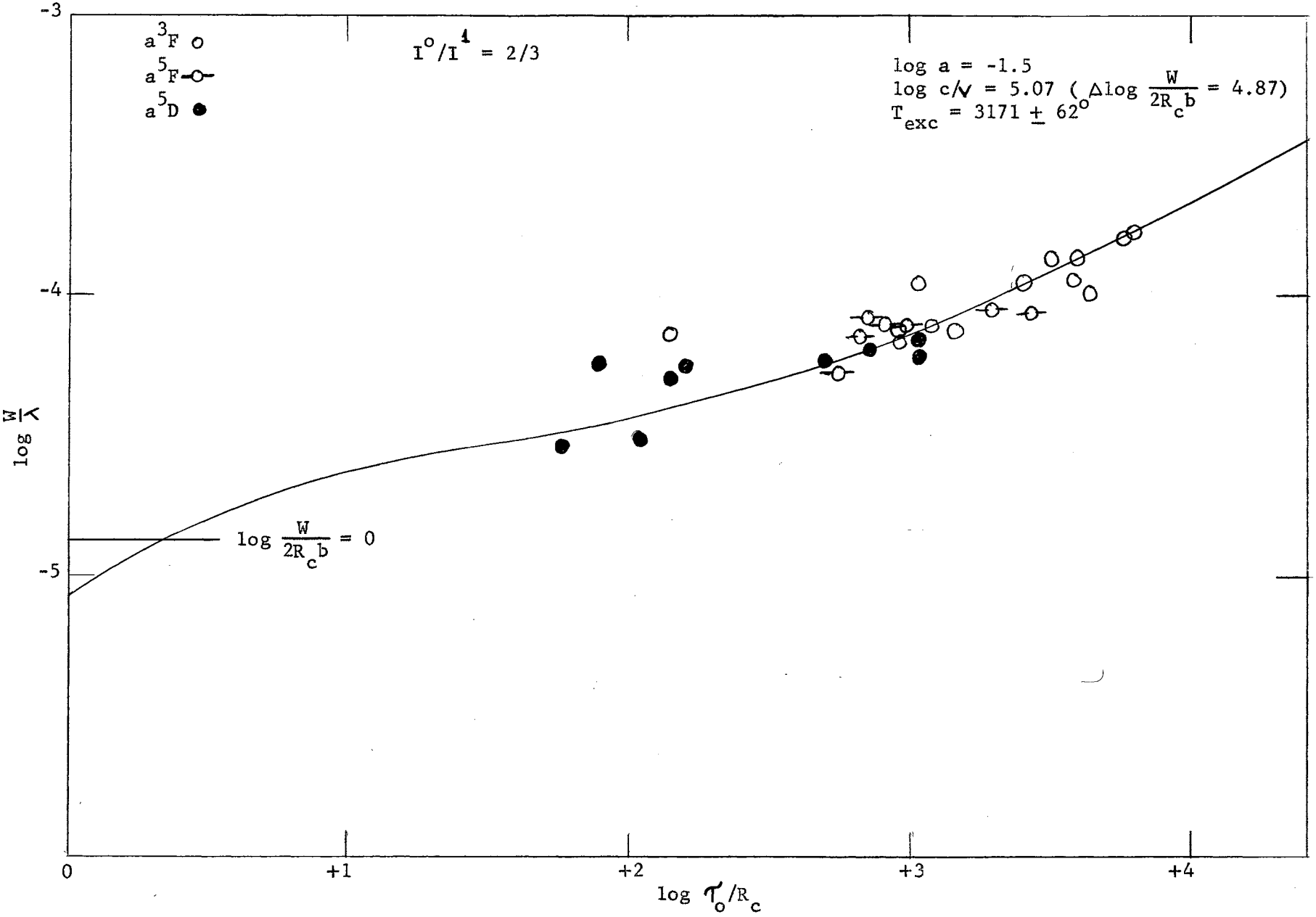

Figure 18. Schuster-Schwarzschild Pure Absorption Curve of Growth for Fe I-King

TABLE IX

CURVE OF GROWTH DATA DERIVED FROM Fe I-CARTER LINES

				M-E Model		S-S Model	
				Scattering	Absorption	Scattering	Absorption
log c/v				5.09	4.98	5.05	4.98
log a				-1.8	-1.0	-1.8	-1.5
Term	χ_e	Measures	Weight	Δ log X	Δ log X	Δ log X	Δ log X
a^5D	0.10	1	0	11.09	10.25	10.66	10.93
a^3F	1.56	4	2	9.00	8.26	8.55	8.78
a^5P	2.19	6	2	7.97	7.15	7.44	7.79
z^7D	2.44	6	3	7.64	6.76	7.33	7.53
b^3P	2.84	2	0	6.93	6.13	6.48	6.72
z^7P^o	2.99	4	1	7.55	6.72	7.10	7.36
c^3P	3.06	1	0	7.30	6.44	6.91	7.16
z^5D	3.20	1	0	7.00	6.23	6.54	6.82
z^5F^o	3.35	3	1	6.99	6.12	6.64	6.86
a^1H	3.56	1	0	6.43	5.55	5.98	6.26
Excitation Temperature (^oK)				4235 $\pm$ 414	3932 $\pm$ 417	4560 $\pm$ 456	4461 $\pm$ 320

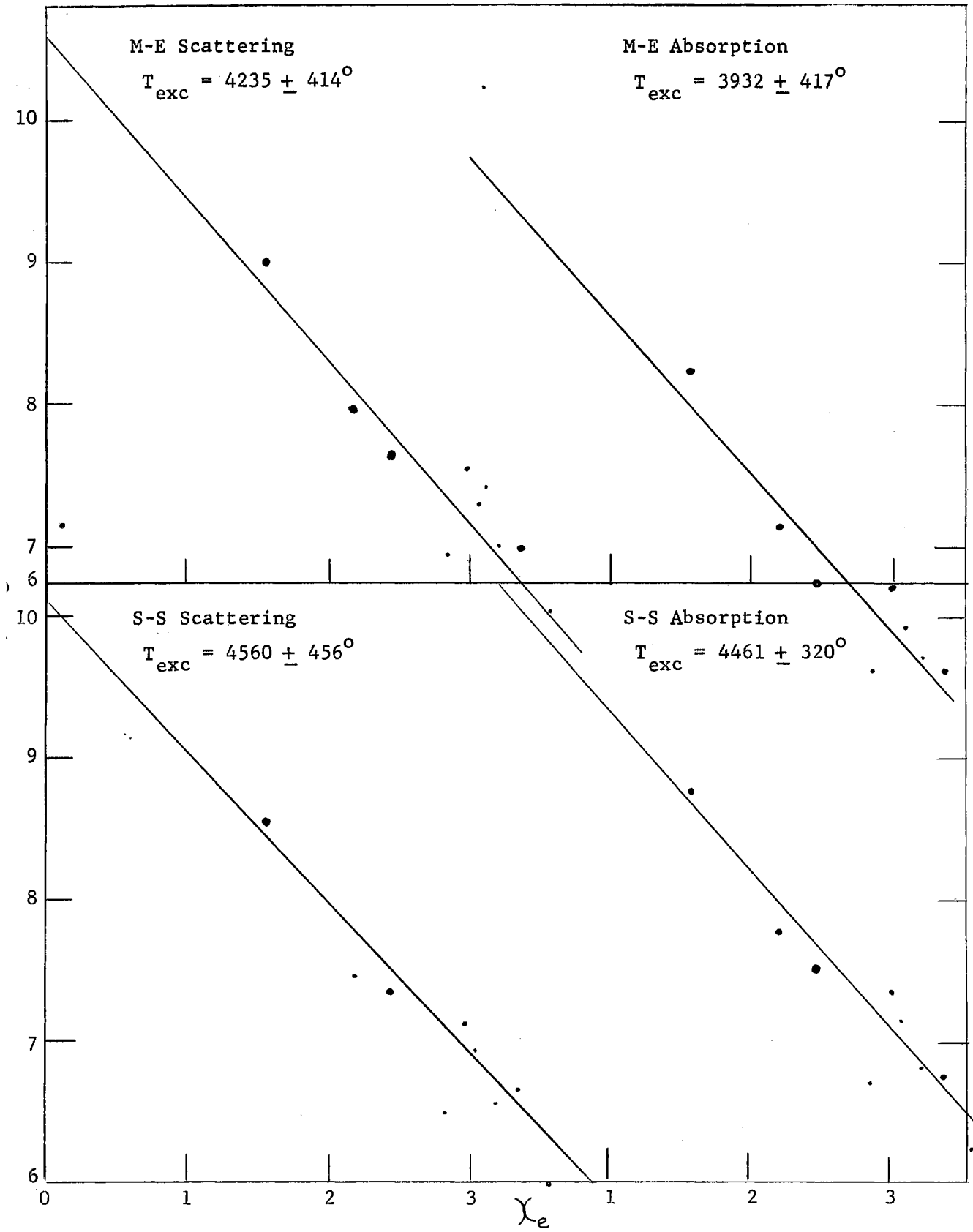

Figure 19. Excitation Temperatures Derived from Fe I-Carter Lines

TABLE X

CURVE OF GROWTH ABUNDANCE DATA FOR Fe I-CARTER

			M-E Model		S-S Model	
			Scattering	Absorption	Scattering	Absorption
log a			-1.8	-1.0	-1.8	-1.5
θ			1.20	1.30	1.12	1.14
log u			1.41	1.39	1.42	1.42
Term	χ_e	Weight	Shift	Shift	Shift	Shift
a^5D	0.10	0	11.21	10.38	10.77	11.04
a^3F	1.56	2	10.87	10.29	10.30	10.56
a^5P	2.19	2	10.60	10.00	9.99	10.29
z^7D^o	2.44	3	10.57	9.93	10.06	10.31
b^3P	2.84	0	10.34	9.82	9.66	9.96
z^7P^o	2.99	1	11.14	10.61	10.45	10.77
c^3P	3.06	0	10.97	10.42	10.34	10.65
z^5D^o	3.20	0	10.84	10.39	10.12	10.47

TABLE X (Cont'd)

Term	χ_e	Weight	Shift	Shift	Shift	Shift
$z\,^5F^o$	3.35	1	11.01	10.48	10.39	10.68
$a\,^1H$	3.56	0	10.70	10.18	9.97	10.32
Weighted Shift			10.76	10.16	10.18	10.45
Abundance		log $N/\rho\bar{\kappa}$	19.38	18.90		
		log NH			18.85	19.00

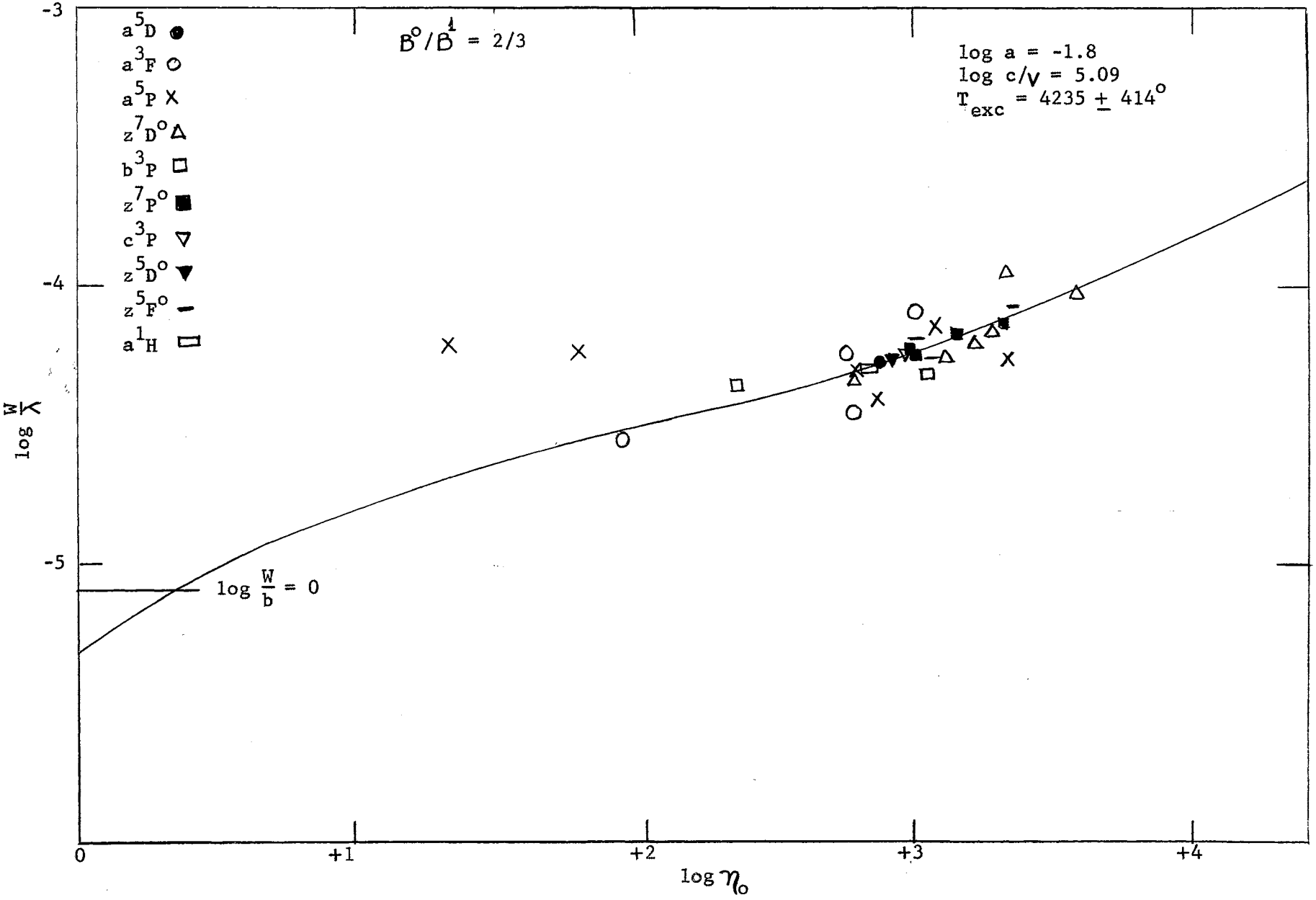

Figure 20. Milne-Eddington Pure Scattering Curve of Growth for Fe I-Carter

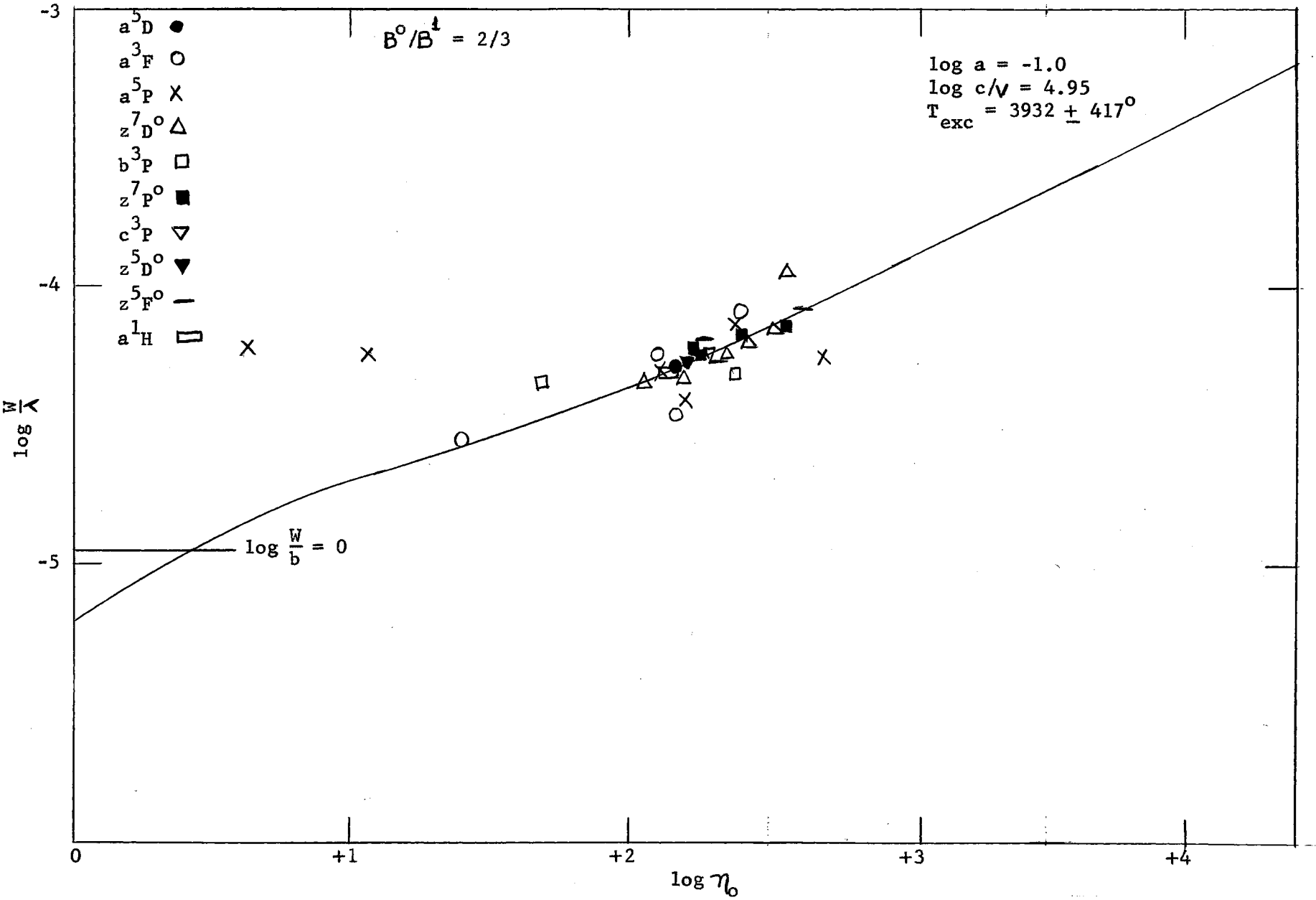

Figure 21. Milne-Eddington Pure Absorption Curve of Growth for Fe I-Carter

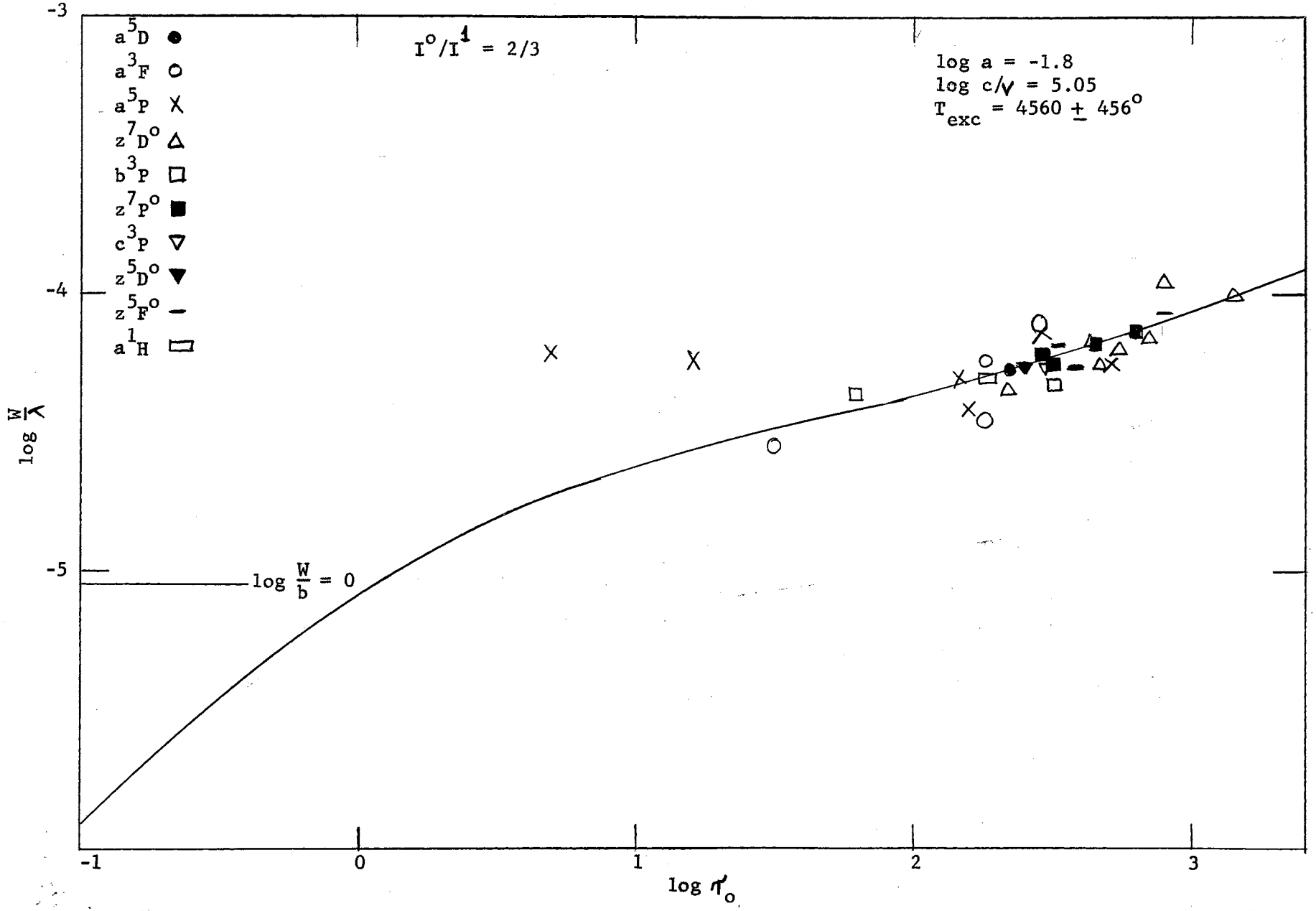

Figure 22. Schuster-Schwarzschild Pure Scattering Curve of Growth for Fe I-Carter

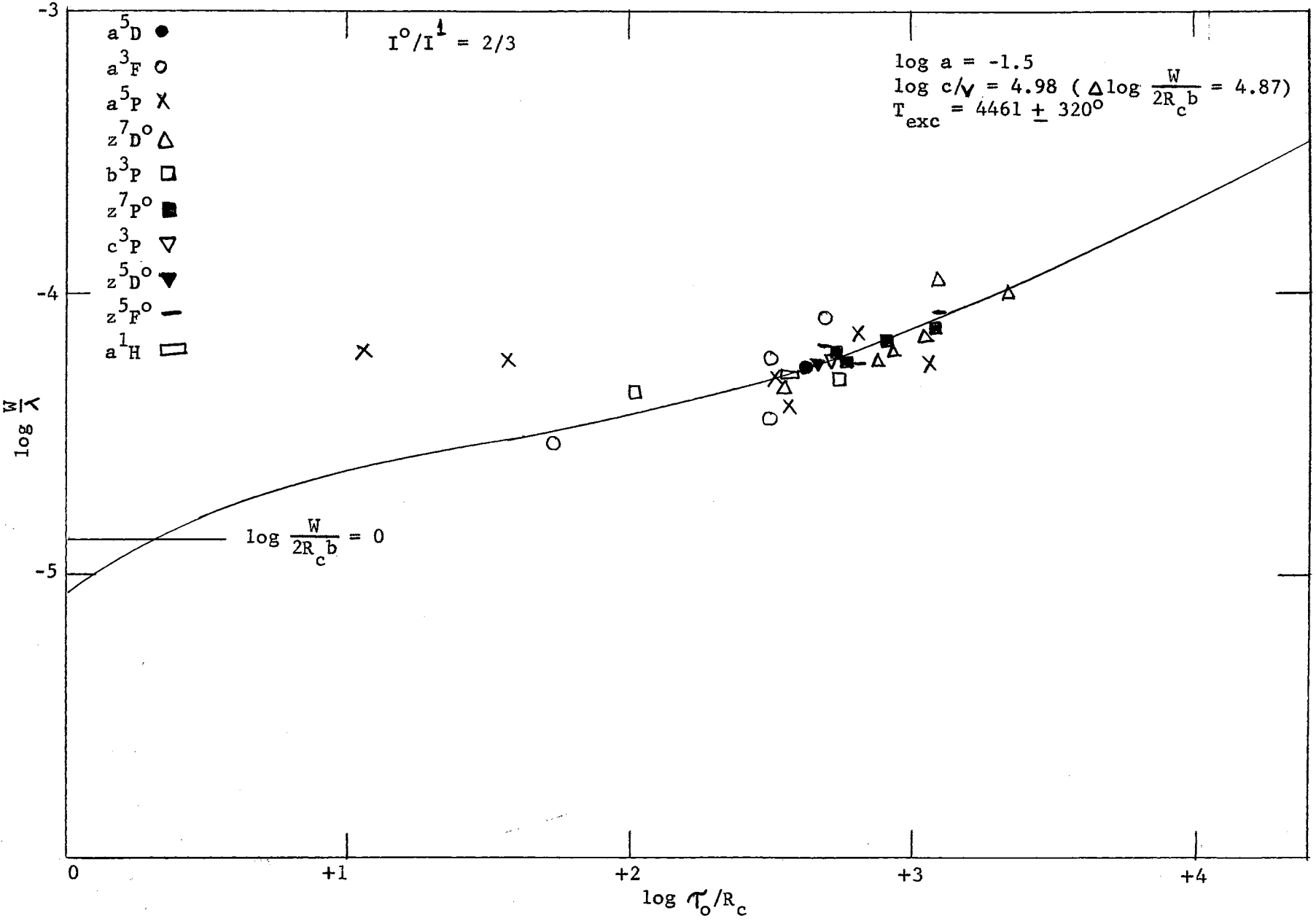

Figure 23. Schuster-Schwarzschild Pure Absorption Curve of Growth for Fe I-Carter

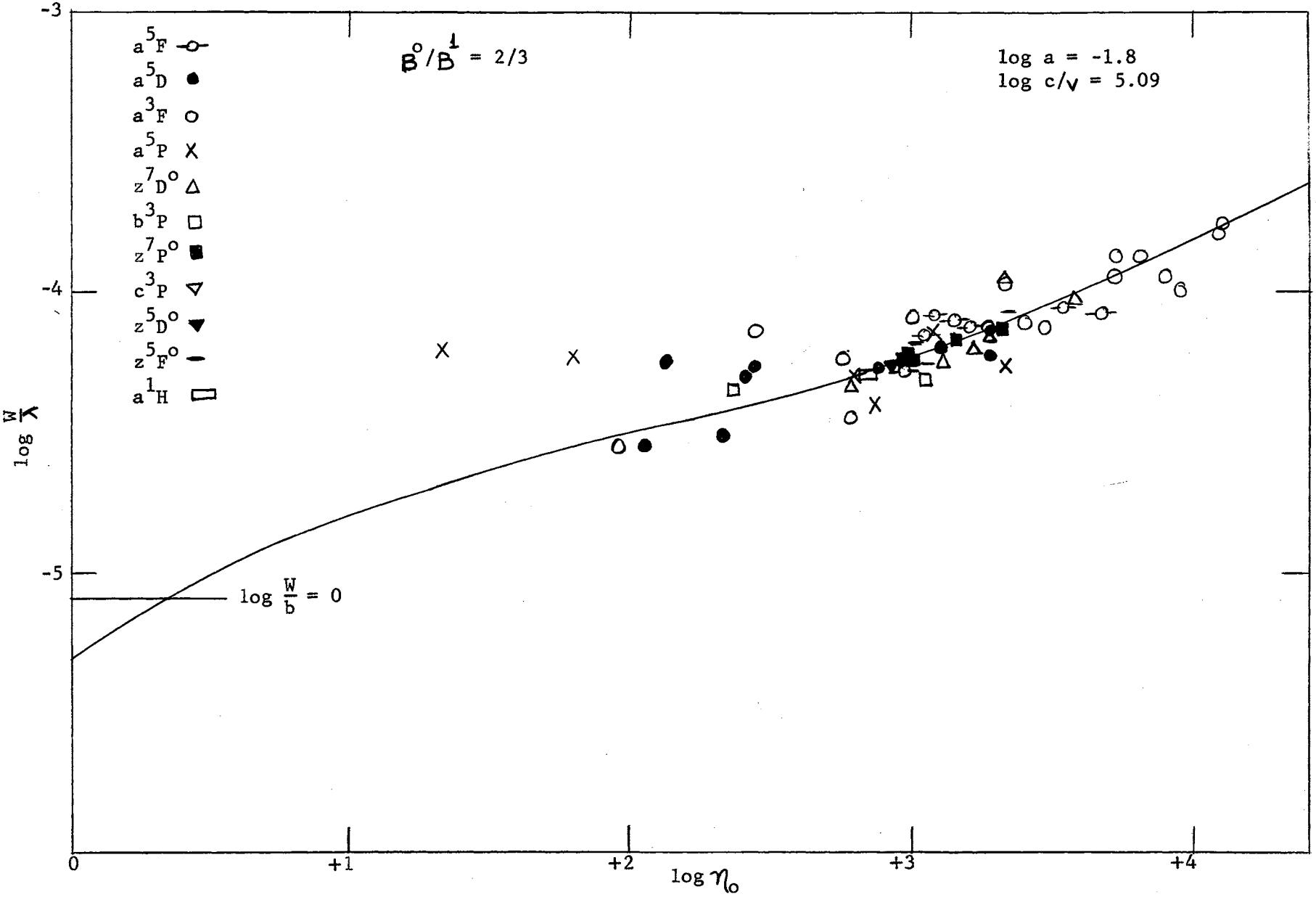

Figure 24. Milne-Eddington Pure Scattering Curve of Growth for Fe I-King and Carter

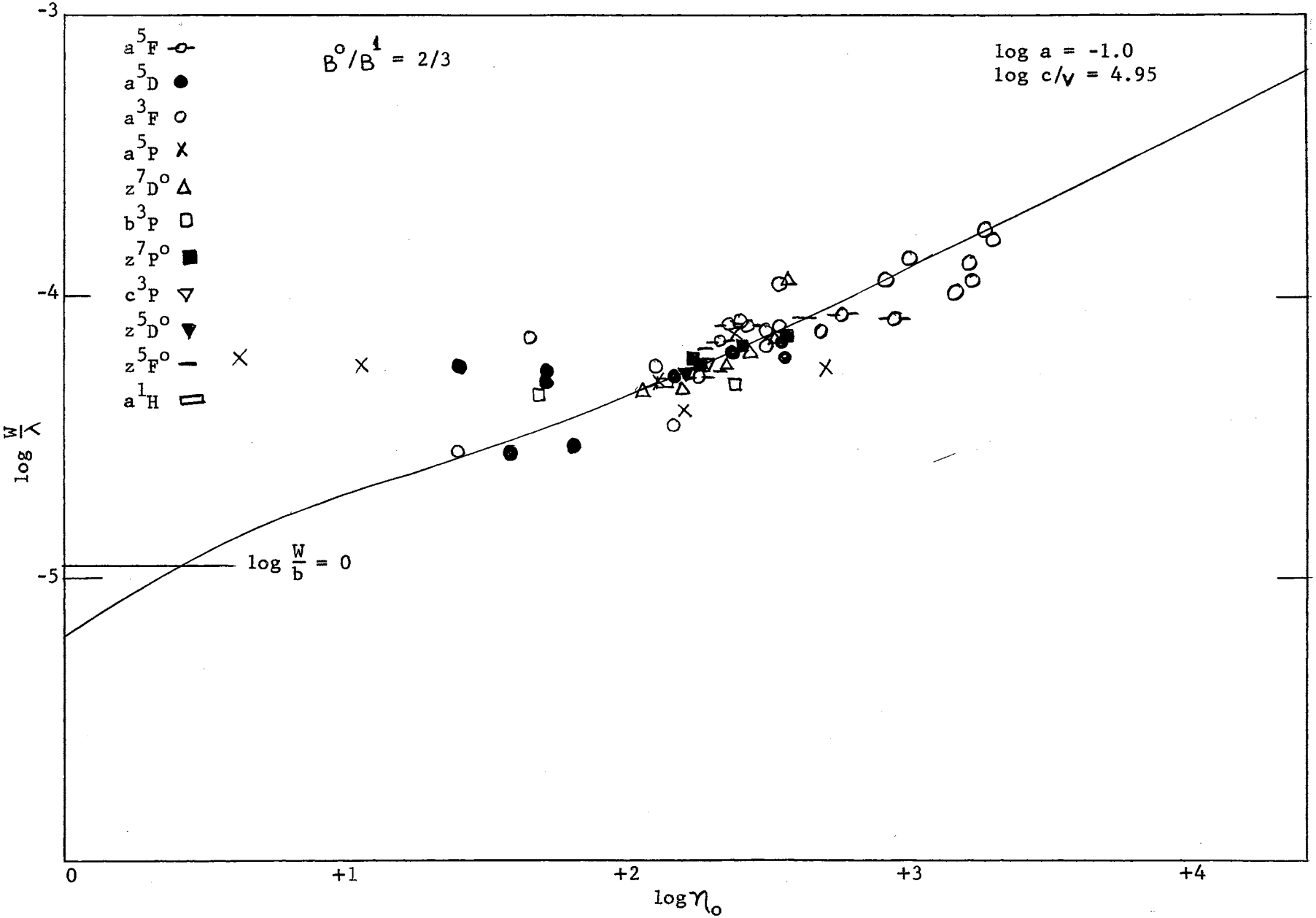

Figure 25. Milne-Eddington Pure Absorption Curve of Growth for Fe I-King and Carter

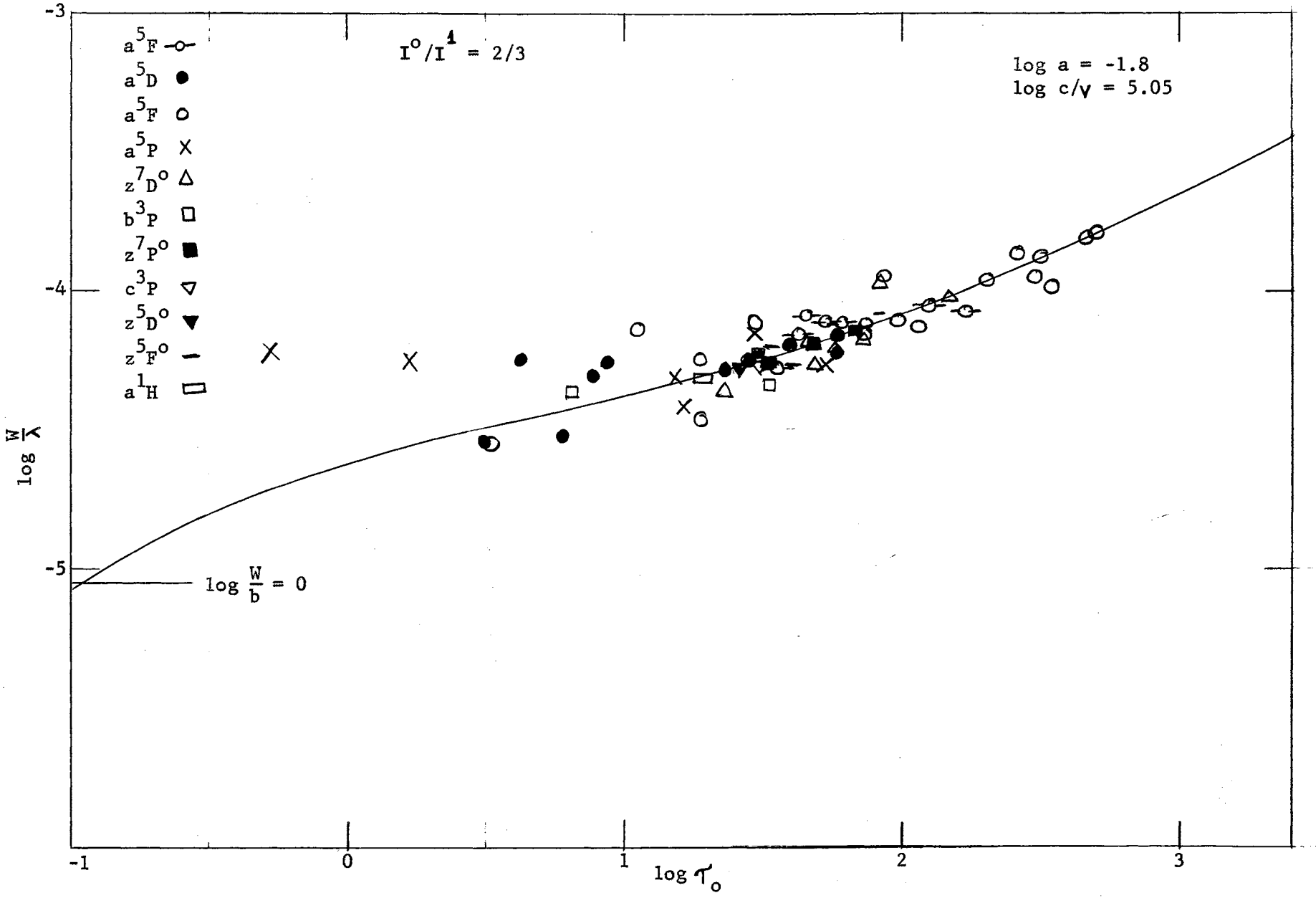

Figure 26. Schuster-Schwarzschild Pure Scattering Curve of Growth for Fe I-King and Carter

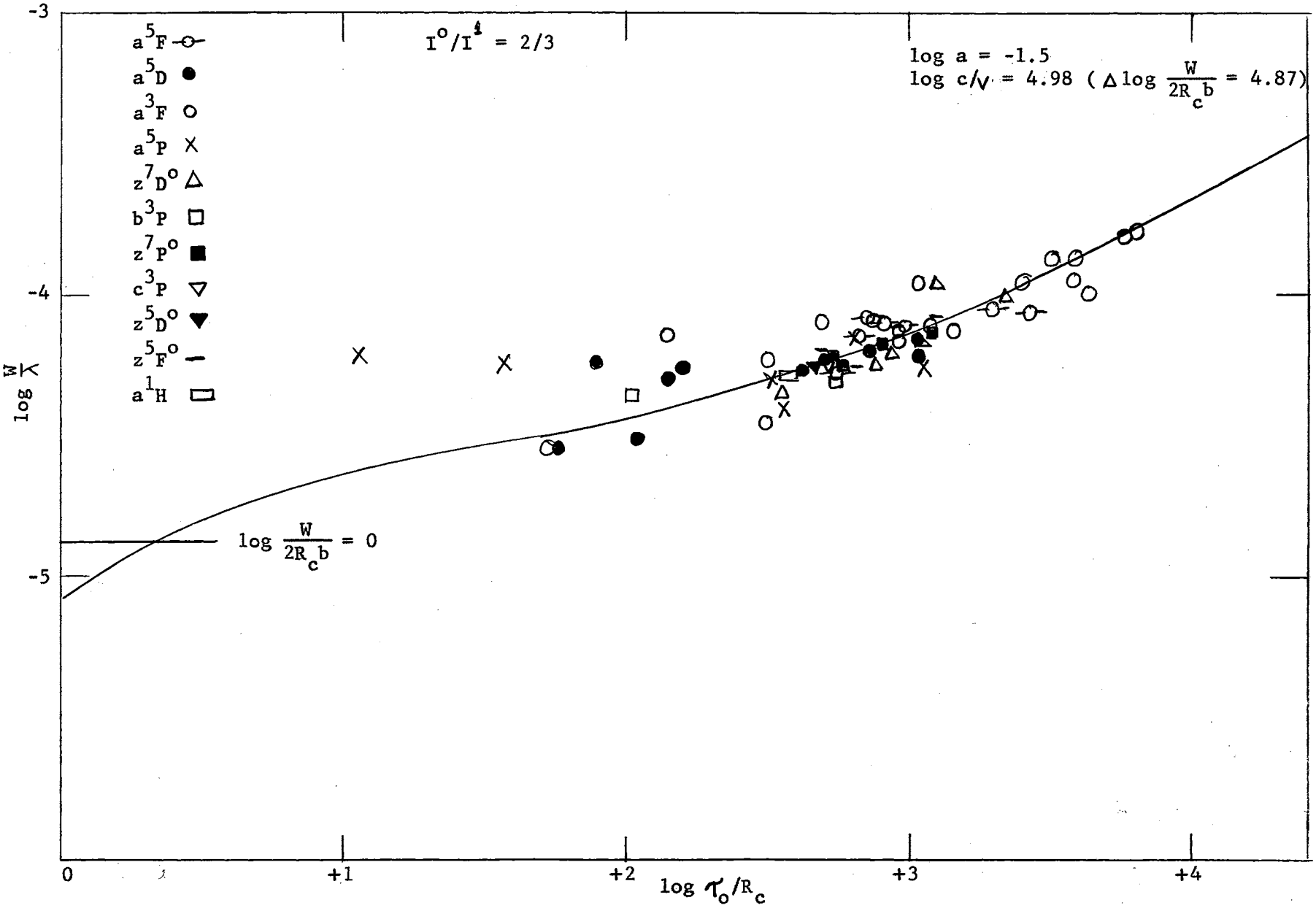

Figure 27. Schuster-Schwarzschild Pure Absorption Curve of Growth for Fe I-King and Carter

VII. CONCLUSIONS

All the results obtained from the curve of growth analyses are summed in Table XI. A discussion of these results follows.

Damping.--In order to get a reliable value for log a at least one multiplet should have many lines covering a wide range of intensities. That is, the multiplet should be such that it fits the theoretical curve both along the flat portion and the damping portion. It has been mentioned that a value of log a was approximated to assist in fitting to the theoretical curves because of the scatter. This was particularly true in the case of Ti I since only a few lines were available. The best which could be done was to choose between possible values predicted by the approximation. The range of intensities was not bad for Ti I as two strong lines were measured. One in the a^5F multiplet and one in the a^3F multiplet. More lines should have more clearly defined the shape of the curve. Due to this scarcity of lines the results determined for Ti I cannot be considered reliable.

In the case of Cr I 15 lines of the a^5D multiplet were measured. Unfortunately none of these were particularly strong and the range of all intensities was rather small. However it is felt that the many lines of this multiplet more clearly defined the choice of the curve fitted than was the case for Ti I. The strongest lines measured belonged to the a^7S multiplet but the scatter was such that they were of little use in choosing the value of log a. Thus the value obtained for Cr I, while

TABLE XI

RESULTS FROM CURVE OF GROWTH ANALYSIS

	log c/v	log a	Excitation Temperature (^{O}K)	log $N/\rho\bar{\kappa}$	log NH	Δ log $N/\rho\bar{\kappa}$ or Δ log NH
M-E Scattering	5.15	-1.4	4536 ± 38	16.49		
M-E Absorption	5.20	-1.0	4588 ± 72	16.42		
Ti I						2.31
S-S Scattering	5.20	-1.4	4979 ± 42		16.24	
S-S Absorption	5.22	-1.5	4861 ± 45		17.01	
M-E Scattering	5.17	-1.4	4339 ± 197	16.77		
M-E Absorption	5.05	-1.0	4317 ± 221	16.42		
Cr I						1.94
S-S Scattering	5.23	-1.4	4212 ± 180		16.66	
S-S Absorption	5.10	-1.5	4238 ± 185		16.92	
M-E Scattering	5.09	-1.8	3256 ± 91	18.82		
M-E Absorption	4.95	-1.0	3180 ± 94	18.12		
Fe I-King						1.19
S-S Scattering	5.05	-1.8	3476 ± 375		18.45	
S-S Absorption	5.07	-1.5	3171 ± 62		18.61	
M-E Scattering	5.09	-1.8	4235 ± 414	19.38		
M-E Absorption	4.95	-1.0	3932 ± 417	18.90		
Fe I-Carter						1.19
S-S Scattering	5.05	-1.8	4560 ± 456		18.85	
S-S Absorption	4.98	-1.5	4461 ± 320		19.00	

perhaps not too accurate, are surely better than those of Ti I. For Fe I-King the a^3F multiplet has a number of measures and the plot was relatively well defined so that the value of log a must be considered quite reliable.

In the case of Fe I-Carter both the a^5P and z^7D^o multiplets had six lines measured. However only the z^7D^o plot was sufficiently defined for use in the choice of log a. This multiplet was particularly good in the choice of log a for the M-E models.

As far as is known no other work has been done on this star which would enable a comparison of values to be made.

Log c/ν.--The same difficulties involved in the choice of log a were encountered here. The reliability of this determination is also the same as mentioned in each case above for log a. Giving equal weights to the value of log c/ν found from each model, the average log c/ν is 5.19 for Ti I, 5.14 for Cr I, and 5.03 for Fe I.

Excitation Temperatures.--The scatter in the various plots made it quite difficult to determine exactly what amount of horizontal shift was needed. Since the value of the excitation temperature is determined by this shift, the more difficult the choice of the horizontal shift the less reliance one can place on the value of the excitation temperature. For Ti I the a^5P multiplet had only one measured line and was valueless in this determination. The scatter of the other two multiplets was very bad and also the intensity was based upon only one observation in many cases. Hence again it must be stated that the value for Ti I is questionable.

Since nearly half of the lines measured for Cr I belonged to a single multiplet and the rest were distributed among several others the

determination of the horizontal shifts were particularly difficult to determine accurately. Here also the lack of observations of the individual lines must be considered as a factor in the reliability of the results.

The Fe I-King values are also open to question due to the large scatter of the a^5D multiplet plot and the poor definition of both the a^5D and a^5F plots. The values are in fair agreement with one another except for the case of S-S scattering for which there was a large probable error.

In the case of Fe I-Carter several multiplets had only one line measured. The horizontal shifts for these were considered completely unreliable and did not enter in the determination of the excitation temperatures. Fitting to the theoretical curves was somewhat simpler and hence the values here should be considered the most accurate.

The apparent disparity between the values of Fe I-King and Fe I-Carter excitation temperatures can be partially explained by the differences in lower level excitation potentials. These ranged from 0.06 to 1.54 for Fe I-King and from 0.10 to 3.56 for Fe I-Carter. However the difference in excitation temperatures averaged about $1000^{\circ}K$. This would appear too large to be completely explained by the excitation potentials and may be in part due to the large scatter of the observations.

Abundances.--In general when one speaks of abundances he thinks either of the total number of particles or objects or the number per unit volume. The "N" which occurs in the curve of growth literature is indeed the number of absorbing atoms per unit volume. This determination is beyond the scope of the curve of growth analysis.

Using the S-S model one obtains log NH where H is height of the reversing layer above the photosphere. To obtain N this quantity H must

be known and cannot be rigorously determined. It varies with excitation, ionization, and from element to element. Then from the S-S model one can only obtain NH, the number of absorbing atoms in a one square centimeter column in the line of sight through the atmosphere above the photosphere.

For the M-E model N/ρ represents the number of atoms per gram of stellar material and $1/\kappa$ is the number of square centimeters per gram. So again only the number per square centimeter is obtained. Further refinement of the theory is needed to obtain only N.

Since no other studies of this star are available for comparison purposes a rough comparison may be made with the results obtained by Schroeder (1958) from the spectrum of Procyon. The lines used in his study are essentially the same as those used here. Of course the results would be expected to vary as the two have different effective temperatures and are of different spectral class and luminosity classification. Procyon is a subgiant of luminosity class IV and spectral class F5.

The only variation in the value of the damping constant is for Ti I, M-E pure absorption. For Procyon log a = -3.0, while for ϵ-Leonis log a = -1.0.

The values of log c/ν found for Procyon run somewhat smaller than those found in this paper. This is the result to be expected. Since ν depends upon the temperature, it would be less for ϵ-Leonis and consequently log c/ν should be greater for ϵ-Leonis.

The greatest variation in results was for excitation temperatures. The average values for the excitation temperatures derived for Procyon are approximately 6000° for Ti I, 4300° for Cr I, 4500° for Fe I-King, and 5000° for Fe I-Carter. This compares with 4700°, 4300°, 3300°, and

4300° found in this paper. Except for Cr I there is considerable variation. The higher intensity of the lines in the spectrum of ϵ-Leonis might have a bearing here.

The abundance determinations for the two stars have about the same relation as the values of log c/v. That is, they run somewhat higher for ϵ-Leonis than for Procyon.

The average value of the logarithms of the abundances from the four models was for Ti I - 16.54, for Cr I - 16.69, for Fe I-King - 18.50, and for Fe I-Carter - 19.03.

It should be stated that the results obtained by any curve of growth analysis can be no more accurate than the determination of the equivalent widths. To increase the accuracy of these a number of measurements of a single line should be made. That is the line should appear on several tracings so that the shape and size could be compared more often. The Ti I results were particularly hampered by a lack in this respect. Another source of error in this determination is small dispersion. Those tracings resulting from the three prism spectrograph had increasingly low dispersion as the wavelength increased. Consequently it was quite easy to make relatively large errors in the size of the profile drawn. The error involved in the drawing in of the continuum is something the investigator must "learn to live with" to use the vernacular. Perhaps the combining of the first three steps in the curve of growth technique will increase the accuracy of this type of analysis. This remains to be seen.

As one last comment a mention should be made as to whether any one model is preferred. From the results of Table XI it would appear that there is little from which to choose. Comparing the curves of growth it is again quite difficult to say although the fit of the M-E pure absorption

for Fe I-Carter seems to be the best and the overall results for Fe I-Carter are felt to be the most reliable. This better fit is likely due to the reduced scatter resulting for the corrections $\Delta \log \eta_o$. Also since the central intensities of the strongest lines are not zero it would seem that absorption would be preferred to scattering as the mode of radiative transfer since zero intensity is predicted here by the theory for scattering.

Further study of the atmosphere of ϵ-Leonis might be worthwhile. Such study should recognize the effects of turbulence upon the curve of growth. Here a value of the velocity due to turbulence, v_T of equation (1), might be assumed and the apparent kinetic temperature, due to this added term, found. This would give the value of T for which the theoretical curve should be drawn. Study by means of model atmosphere calculations and line profile studies together with the results of this paper might give a more comprehensive and definitive view of the atmosphere of ϵ-Leonis.

SELECTED BIBLIOGRAPHY

Allen, C. W. "Astrophysical Quantities". London: Atholone Press, 1955.

Aller, L. H. "Atmosphere of the Sun and Stars". New York: Ronald Press, 1953.

_____. "Atmospheres of the B Stars. I. The Supergiant Epsilon Canis Majoris". Ap. J. 123, 117-131 (1956).

Bell, G. D., R. P. King and P. M. Routly. "The Absolute f-Values of λ3237 of Cu I and λ3720 of Fe I". Ap. J. 127, 775-796 (1958).

Carter, W. W. "Measurement of f-Values in the Iron Spectrum with Applications to Solar and Stellar Atmospheres". Phys. Rev. 76, 962-966 (1949).

Claas, W. J. "The Composition of the Solar Atmosphere". Rech. Astr. Obs. Utrecht. Vol. 12, Part I, pp. 49-50.

Hill, A. J. and R. B. King. "Relative f-Values for Lines of Cr I". J. O. S. A. 41, 315-321 (1951).

Houtgast, J. "The Variations in the Profiles of Strong Fraunhofer Lines Along a Radius of the Solar Disc". Utrecht: Schotanus & Sons, 1942.

Hunger, K. "Zur Theorie der Wachstumskurven". Zs. f. Ap. 39, 36-60 (1956).

Keenan, P. C. and W. W. Morgan. "Astrophysics: A Topical Symposium". New York: McGraw & Hill, 1951, p. 15.

King, R. B. and A. S. King. "Relative f-Values for Lines of Fe I and Ti I". Ap. J. 87, 24-39 (1938).

Menzel, D. H. "The Theoretical Interpretations of Equivalent Breadths of Absorption Lines". Ap. J. 84, 462-473 (1936).

Schroeder, L. W. Doctoral Thesis, Indiana University, 1958. (Unpublished).

Stromgren, B. "The Boundary Value Problem of the Theory of Stellar Absorption Lines". Ap. J. 86, 1-27 (1937).

Swensson, J. "The Spectrum of Procyon: A Typical Star of Class F". Ap. J. 103, 207-248 (1946).

Thackeray, A. "Intensities of Blended Absorption Lines". Ap. J. 84, 433-461 (1936).

Wright, K. O. "A Study of Line Intensities in the Spectra of Four Solar-Type Stars". Pub. Dom. Ap. Obs. Victoria. VIII No. 1.

_____. "Line Intensities in the Spectra of K-Type Stars I Alpha Bootis and Gamma Draconis". Ibid. VIII No. 9.

Wrubel, M. H. "Exact Curves of Growth for the Formation of Absorption Lines According to the Milne-Eddington Model. I. Total Flux". Ap. J. 109, 66-80 (1949).

_____. "Exact Curves of Growth for the Formation of Absorption Lines According to the Milne-Eddington Model. II. Center of the Disk". Ibid. 111, 157-164 (1950).

_____. "Exact Curves of Growth. III. The Schuster-Schwarzschild Model". Ibid. 119, 51-57 (1954).

_____. 1956 (unpublished).

VITA

Ray Lewis Fisher

Candidate for the Degree of

Master of Science

Thesis: A STUDY OF LINE INTENSITIES IN THE SPECTRUM OF ϵ-LEONIS

Major Field: Physics

Biographical:

Personal Data: Born at Muskogee, Oklahoma, May 18, 1932, the son of William J. and Jonnie B. Fisher. Married November, 1957 to the former Imogene Green. Sons Jeffry and Brian born August, 1958 and August, 1960, respectively.

Education: Elementary, junior high and high school education received at Muskogee, Oklahoma. Graduated from Muskogee Central High School May, 1950. Freshman year of college spent at Muskogee Junior College. Received Bachelor of Science degree in Physics from Oklahoma State University in May, 1954.

Professional Experience: Employed by Humble Oil and Refining Co. upon graduation in 1954 as a seismic operator. Resigned position in June, 1959 to return to this institution for graduate work.